Russian Geology and Geophysics © 2020, V.S. Sobolev IGM, Siberian Branch of the RAS
Vol. 61, No. 4, pp. 378–395, 2020 *DOI:10.15372/RGG2019149* *Geologiya i Geofizika*

The Chukotka Segment of the Uda–Murgal and Okhotsk–Chukotka Volcanic Belts: Age and Tectonic Environment

P.L. Tikhomirov[a,b,] ✉, N.V. Pravikova[a], Ya.V. Bychkova[a]

[a] *Lomonosov Moscow State University, Leninskie Gory 1, Moscow, 119991, Russia*

[b] *North-East Interdisciplinary Scientific Research Institute, Far Eastern Branch of the Russian Academy of Sciences, ul. Portovaya 16, Magadan, 685000, Russia*

Received 15 October 2018; received in revised form 23 January 2019; accepted 28 August 2019

Abstract—We present new data on the geology, geochronology, and geochemistry of volcanic complexes of the Uda–Murgal and Okhotsk–Chukotka belts that expose on the left bank of the Anadyr' River in its middle course. The structural relationships between the stratons, supplemented by the U–Pb and $^{40}Ar/^{39}Ar$ dates of volcanics, indicate at least three compression events at this segment of the Pacific margin during the Cretaceous: pre-Aptian, early Albian, and late Turonian. The complexes of the Uda–Murgal and Okhotsk–Chukotka belts are separated by an early Albian unconformity, but the other two unconformities are also well pronounced. The studied segment of the Uda–Murgal belt evolved in the ensialic island arc setting till the Barremian. In the Aptian, after the accretion of the island arc to the continent, volcanism reactivated on the Andean-type margin. The main geochemical difference between the Uda–Murgal and Okhotsk–Chukotka belts is the different volume portions of silicic rocks. The less significant difference in the contents of trace elements indicates a change in the composition of the mantle protolith. The complexes of the Okhotsk–Chukotka belt show signs of geochemical zoning, both longitudinal and transverse relative to the strike of the continent–ocean boundary.

Keywords: magmatism, geochronology, geochemistry, northeastern Asia, Uda–Murgal belt, Okhotsk–Chukotka belt

INTRODUCTION

Jurassic–Cretaceous magmatic belts are a significant part of the East Eurasian geologic structure. A system of such belts is traceable for at least 8000 km from Hainan Island to the eastern coast of the Chukchi Peninsula (Khanchuk, 2006; Zhou et al., 2015). The huge volcanic output and the high metal potential of corresponding magmatic provinces expectedly attract the attention of researchers: Hundreds of research works have been dedicated to the geology, petrology, and metallogeny of Jurassic–Cretaceous volcanic belts of eastern Eurasia. In the near decade, the studies of these volcanic provinces will probably escalate owing to the commercial exploitation of ore deposits and the development of analytical technique.

The Okhotsk–Chukotka volcanic belt (OCVB) is the largest in East Asia and perhaps the largest of all Phanerozoic continental-margin volcanic belts. This geologic structure is more than 3000 km in length; the present-day outcrop area of its volcanic complexes (excluding eroded ones) approaches 400,000 km^2. In the 1960–1970s, the OCVB was considered a typical "marginal volcanic belt" (Bogdanov, 1965). Later on, after the adoption of the plate tectonics paradigm, it was regarded as an Andean-type suprasubductional belt (Parfenov, 1984; Nokleberg et al., 2001).

During the sixty years that have passed since the publication of the first reviews of the OCVB geology (Ustiev, 1959, 1963), the concepts of the age of this province changed significantly. Some researchers believed that the OCVB formed throughout the entire Cretaceous (Ustiev, 1963; Shpetnyi et al., 1974; Umitbaev, 1986), whereas others limited its age to the Albian–Cenomanian period (Belyi, 1975, 1988). According to the current models constructed from the results of U–Pb and $^{40}Ar/^{39}Ar$ dating of igneous rocks (Akinin and Miller, 2011; Tikhomirov et al., 2012), the OCVB formed in the time interval 106–74 Ma (Albian–Campanian, according to Ogg et al. (2008)).

In the 1980s, it was proposed to exclude the Upper Jurassic and Lower Cretaceous (pre-Albian) volcanic strata from the OCVB. These strata accumulated mostly in the subaqueous environment, and they are separated from the younger subaerial volcanics by an unconformity. The geologic structure that comprises the Upper Jurassic and Lower Cretaceous volcanics and comagmatic intrusive rocks is called the Uda–Murgal volcanic belt (UMVB), or volcanic arc (Parfenov, 1984; Filatova, 1988). The overview of the stratigraphy and tectonic structure of the UMVB is presented in a series of publications (e.g., Goryachev, 2005; Belyi, 2008; Sokolov et al., 2009; Rusakova, 2011). However, the infor-

✉ Corresponding author.
E-mail address: petr_tikhomirov@mail.ru (P.L. Tikhomirov)

mation about the chemical composition of the UMVB rocks is rather limited and dominated by major element data. The trace-element contents and isotope ratios were determined only in several rock samples (Sokolov et al., 2009; Akinin and Miller, 2011), and these data are far from being sufficient for the igneous province more than 2500 km in length. The U–Pb and $^{40}Ar/^{39}Ar$ dates for the UMVB igneous rocks are also scarce (Bondarenko et al., 1999; Luchitskaya et al., 2003; Akinin and Miller, 2011). The paucity of precise analytical data hampers the understanding of the history and dynamics of the UMVB, including issues of its initiation, activity variations, and comparison between the sources of the UMVB and OCVB magmas.

The results of the research carried out in 2008–2010 at the northern segment of the Uda–Murgal belt, in the basin of the Ubienka River (a left tributary of the Anadyr' River), contribute to the solution of the above problems. The research included structural observations, sampling, and laboratory procedures (petrographic study, U–Pb dating of zircons and $^{40}Ar/^{39}Ar$ dating of biotite, and whole-rock analyses for major and trace elements).

AN OVERVIEW OF THE GEOLOGY OF THE UBIENKA RIVER BASIN

The study area lies near the southeastern boundary of the Anadyr' segment of the OCVB (Fig. 1), where the UMVB complexes expose from under the gently dipping OCVB volcanics and the tuffaceous sedimentary rocks of the OCVB

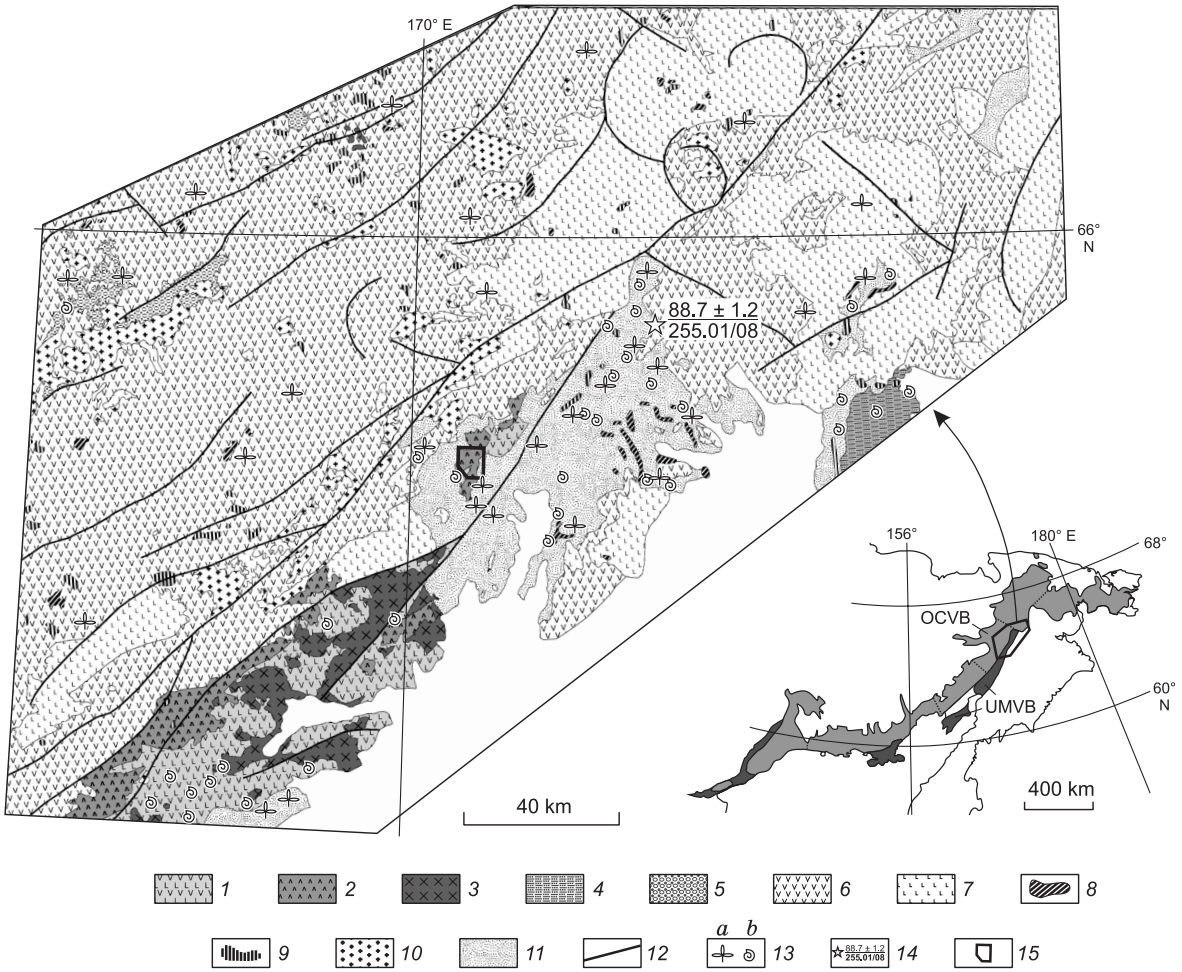

Fig. 1. Geological sketch map of the left side of the Anadyr' River in its upper and middle courses, compiled on the basis of the geological map on a scale of 1:1,000,000 (Malysheva et al., 2012), modified and supplemented. *1–3*, complexes of the Uda–Murgal volcanic belt: *1*, Travka, Yaranga, and Usova formations; *2,* East Berezovaya Formation; *3*, granitic plutons of the Murgal complex; *4*, UMVB forearc basin sequences (Chakhmatkuul', Orlovka, and Chashchevitaya formations); *5*, postcollisional basins of the Oloi zone (Chimchememel' Formation); *6–10*, igneous rocks of the Okhotsk–Chukotka belt: *6*, volcanics of intermediate and silicic composition, *7*, basalts and bimodal basalt–rhyolite sequences of the upper part of the OCVB section (Enmyvaam and Chuvanskaya formations), *8–9,* subvolcanic intrusions (*8*, intermediate and mafic, *9*, silicic), *10*, granitic plutons of the Yablon, Eropol, and Kavral'yanskaya complexes; *11*, OCVB forearc basin (Krivorechenskaya, Dugovaya, Krestovaya, and Pastbishchnaya formations); *12,* major faults; *13*, localities for plant fossils (*a*) and fossil fauna (*b*); *14*, sampling locality for $^{40}Ar/^{39}Ar$ dating: age, Ma (numerator) and sample number (denominator); *15*, outlines of the area shown in Fig. 3. Inset: location of the UMVB (dark-colored) and OCVB (light-colored) relative to the coastline of northeastern Russia. Dash lines depict the boundaries of the OCVB segments.

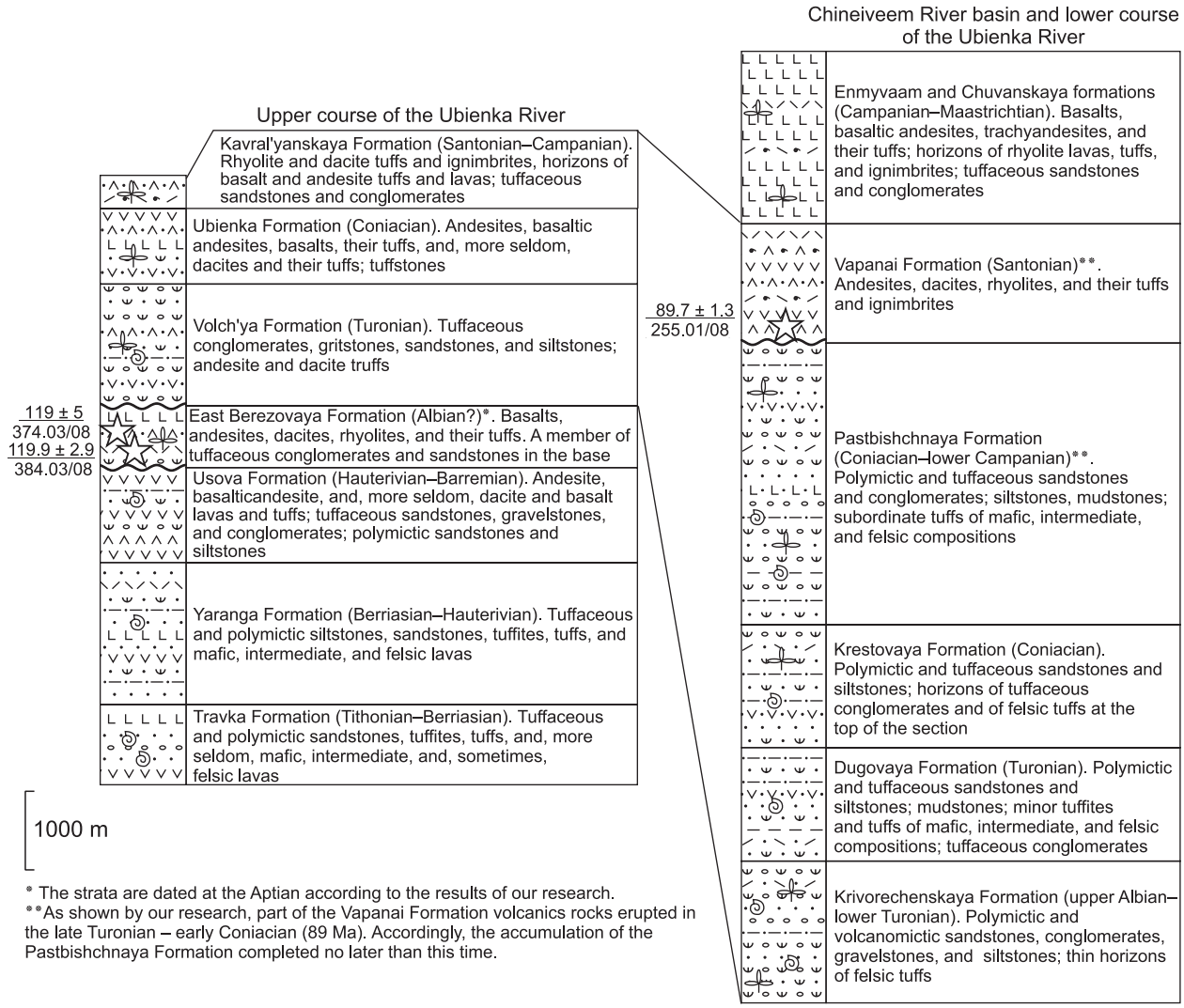

Fig. 2. Stratigraphic scheme of the Cretaceous sequences of the Ubienka River basin (Resolutions..., 2009; Malysheva et al., 2012). The height of the cells corresponds to the maximum thickness of units. Asterisks mark the position of samples used for isotope dating (age, Ma (±2σ) as a numerator and sample number as a denominator). The data on the fossil plants and invertebrates are after Malysheva et al. (2012).

forearc basin. Here, the UMVB rocks compose the small (~30×10 km) Ubienka uplift, the very northeastern part of the Uda-Murgal belt. Late Jurassic and Early Cretaceous complexes were also found further north from this structure, within the Chukotka block, but they are believed to be related to other subduction systems here (Morozov, 2001; Tikhomirov et al., 2008).

The stratigraphic scheme for the northern UMVB and overlying OCVB volcanics is presented in Fig. 2. Three lower units (Travka, Yaranga, and Usova formations) are considered to be related to the UMVB. These units contain fossil bivalves and ammonites of Tithonian–Barremian age (Malysheva et al., 2012). The affinity of the East Berezovaya Formation, which is separated from the underlying sequences by a clear angular unconformity (sometimes, with a horizon of basal conglomerates), remained uncertain until the recent study. In the latest version of the geological map of 1:1,000,000 scale (Malysheva et al., 2012), the East Berezovaya Formation is presumably dated at the Early–Middle Albian and considered among the lowermost units of the OCVB.

The age of the OCVB strata unconformably overlying the UMVB complexes (Volch'ya, Kavral'yanskaya, and Ubienka Formations) is substantiated by findings of Coniacian–Campanian fossil flora (Resolutions..., 2009). The tuffaceous sedimentary formations of the OCVB forearc basin (Krivorechenskaya, Dugovaya, Krestovaya, and Pastbishchnaya), which outcrop in the southeast of the study area (Fig. 1), reveal a much wider time interval, from late Albian to early Campanian. The OCVB volcanics are intruded by several epizonal plutons (up to 100 km^2) dominated by quartz monzonites and granites. At least one of these plutons (Ol'khovka) hosts porphyry copper mineralization (Malysheva et al., 2012).

Within the Murgal uplift, 20–30 km southwest of the study area, the UMVB strata are gently folded, with bedding dip angles of 10 to 40° (Lobunets and Kuznetsova, 1977; Nevretdinov, 1985). The OCVB strata are almost undeformed; their dip angles seldom exceed 15°. The paleotopography and caldera tectonics were probably the major factors that affected the spatial orientation of the volcanic strata of the OCVB. The forearc basin sequences formed synchronously with the OCVB strata, but they are folded, with fold axes nearly parallel to the strike of the volcanic belt (Trunov, 1977). These sequences dip mainly at 10–20° (up to 70° in some fault zones). On the left side of the Ubienka River and in the Chineiveem River basin, the folded strata of the forearc basin are unconformably overlain by a gentle (≤10°) monocline composed of virtually undeformed volcanics of the Vapanai and Enmyvaam formations. These volcanics are commonly associated with the late stage of the OCVB formation (Belyi and Belaya, 1998). The Coniacian–Campanian (ca. 87–74 Ma) age of these formations is constrained by findings of fossil plants and their relation with the paleontologically dated forearc sequences (Malysheva et al., 2012).

FIELD OBSERVATIONS AND SAMPLING

The field study carried out within the area of the Ubienka uplift in 2008 revealed that the UMVB complexes here comprise two major units, strongly different from each other both structurally and lithologically (Fig. 3):

(1) The lower part of the accessible section is marine polymictic and tuffaceous sandstones and siltstones intercalating with lavas and tuffs of basalts, basaltic trachyandesites, and trachyandesites. These rocks compose a monocline dipping at 50 to 70º (probably, a fold limb). The sedimentary horizons contain remains of Tithonian Buchias. This unit may be readily identified as related to the Travka Formation.

(2) The rocks of the Travka Formation are unconformably overlain by subaerial volcanics of variable composition, from basalts to trachydacites and trachyrhyolites, with minor interbeds (up to 10 m thick) of tuffaceous conglomerates. The volcanic sequence dips to the east, northwest, and north at angles of 10 to 20º (Fig. 3). This unit has been identified as part of the East Berezovaya Formation, based on its lithology and clear unconformity with the Travka Formation.

The area of the Ubienka uplift lacks any sequences that could be surely assigned to the Yaranga or Usova formations, the significant constituents of the Murgal segment of the UMVB. To the east, the East Berezovaya Formation is overlain (with a slight inconformity) by the tuffaceous conglomerates and sandstones of the Krivorechenskaya Formation of the OCVB forearc basin.

Three samples of the UMVB volcanics were selected for isotope dating: (1) porphyritic dacite collected within the block composed by the Travka Formation, (2) dacitic crystal

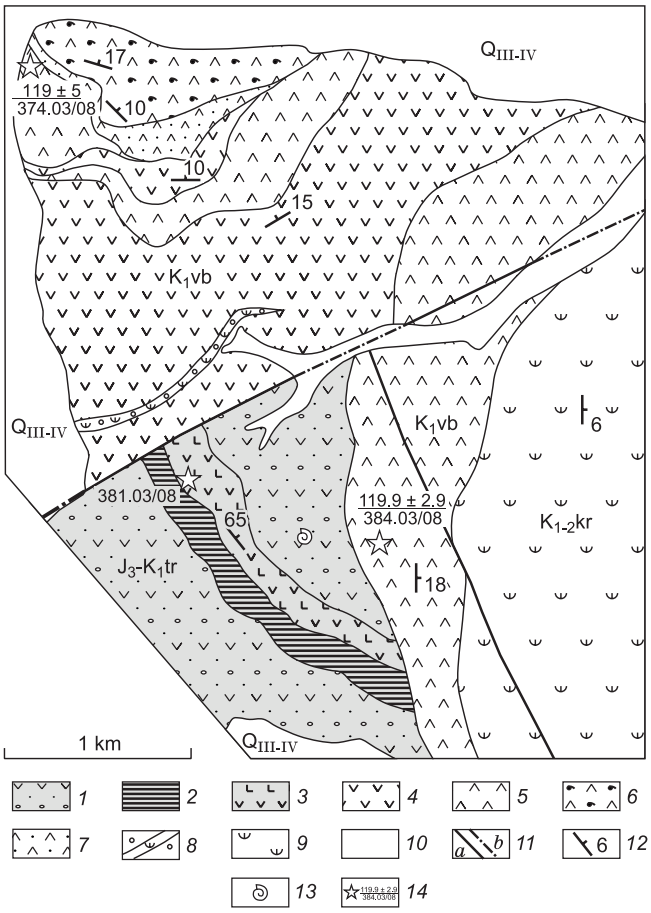

Fig. 3. Geological sketch map of the area of detailed study (the right side of the Pravaya Ubienka River). The location of the area is shown in Fig. 1. *1–3*, Travka Formation, J_3–K_1tr (Tithonian–lower Berriasian): *1*, polymictic and tuffaceous sandstones, siltstones, and conglomerates with minor lavas of basalts and andesites, *2,* tuffaceous sandstones intercalating with lavas of basalts and andesites, *3*, lavas of basalts and andesites, polymictic and tuffaceous sandstones, siltstones, and gravelstones; *4–8*, East Berezovaya Formation, K_1vb (Aptian): *4*, lavas of andesites with thin interbeds of tuffaceous sandstones, *5*, dacitic lavas, *6*, dacitic ignimbrites, *7*, dacitic lithic crystal ignimbrites and tuffs, *8*, tuffaceous conglomerates; *9*, Krivorechenskaya Formation K_{1-2}kr (Albian–Turonian), tuffaceous conglomerates and sandstones; *10*, Quaternary sediments (alluvial, glacial, and fluvioglacial); *11*, faults (*a*, proved, *b*, concealed beneath Quaternary sediments); *12*, dip and strike of strata; *13*, locality of fossil invertebrates; *14*, sampling localities for U–Pb zircon dating (age, Ma (±2σ) as a numerator and sample number as a denominator).

ignimbrite from the East Berezovaya strata, and (3) lava of porphyritic trachyrhyolite of the East Berezovaya Formation. To constrain the age of the local OCVB units, a sample of porphyritic dacite lava was collected from the Vapanai Formation. The sampling localities and the stratigraphic position of the samples are shown in Figs. 1–3. After the preliminary examination of thin sections, 26 samples were chosen for a geochemical study. These samples represent the volcanic strata of the Ubienka uplift and its vicinity. In total, five samples from the Travka Formation, eleven samples from the East Berezovaya Formation, four samples from the

Ubienka Formation, and six samples from the Kavral'yanskaya Formation were selected. Also, we analyzed five samples of the OCVB volcanics collected 40–70 km north of the Ubienka uplift, in the basin of the Chineiveem River. These rocks belong to the Vapanai and Emuneret formations, which are nearly coeval with the Ubienka and Kavral'yanskaya formations (Resolutions..., 2009). The coordinates of all sampling localities are given in Tables 1 and 2.

ANALYTICAL TECHNIQUE

The laboratory studies included examination of thin sections, major- and trace-element analyses, extraction of zircon and biotite and their subsequent isotope dating (U–Pb SHRIMP for zircon and $^{40}Ar/^{39}Ar$ for biotite).

Zircons were separated using standard techniques including heavy-liquid extraction and manual selection. Cathodoluminescence (CL) imaging of zircons shows their likely magmatic nature and the lack of inherited cores. Zircons from the same rock sample have a similar shape and color, without any apparent subpopulations. U–Pb isotope analysis was performed using a SHRIMP-II ion microprobe at the Center of Isotope Research of the Russian Geological Research Institute, St. Petersburg, following the technique described by Larionov et al. (2004). The primary oxygen beam current was 1.5–2.2 nA, the accelerating voltage of secondary oxygen ions was 10 kV, and the analyzed spot was 10×15 μm in size. Before the analysis, a 20×30 μm spot was treated with an oxygen ion beam for 2 min to minimize the possible surface contamination with common lead. Every fourth measurement was performed on the standard sample 91500 with a uranium content of 81.2 ppm and a $^{206}Pb/^{238}U$ age of 1065.4 ± 0.3 Ma (Wiedenbeck et al., 1995). The parts of zircon grains relatively dark in CL images were considered preferable for analysis. The obtained data were processed using the SQUID 1.12 (Ludwig, 2005a) and ISOPLOT/Ex 3.22 (Ludwig, 2005b) software. Ages were calculated using decay constants from Steiger and Jager (1977).

For $^{40}Ar/^{39}Ar$ dating, a biotite sample was manually selected under a binocular microscope. The analysis was performed at the Institute of Geology and Mineralogy, Novosibirsk (analyst A.V. Travin). The sample was irradiated with a fast-neutron flux in a research VVR-K reactor at the Research Institute of Nuclear Physics, Tomsk. The neutron flux gradient did not exceed 0.5% at the sample size. The standard muscovite sample MCA-11 with an age of 313.8 ± 9 Ma was used as a monitor. The sample was dated by step heating method in a quartz reactor with a low-inertia external heating furnace (Travin et al., 2009). Before the measurement, the sample was degassed at 150 ºC. The laboratory blank contamination by ^{40}Ar (determined after heating at 1200 ºC for 10 min) did not exceed $5 \cdot 10^{-10}$ ncm^3. The released argon was cleaned with Ti and ZrAl SAES getters. Its isotope composition was measured on a Noble Gas 5400 mass spectrometer (Micromass, Great Britain). Correction for ^{36}Ar, ^{37}Ar, and ^{40}Ar produced during Ca and K irradiation was made using the following coefficients: $(^{39}Ar/^{37}Ar)_{Ca}$ = 0.000730 ± 0.000026, $(^{36}Ar/^{37}Ar)_{Ca}$ = 0.000320 ± 0.000021, and $(^{40}Ar/^{39}Ar)_K$ = 0.0641 ± 0.0001. The age spectrum was interpreted using the criteria from Fleck et al. (1977) and Gustafson et al. (2001).

The major-element contents were determined by the XRF method with a Philips PW 1600 spectrometer at the Institute of Geochemistry and Analytical Chemistry, Moscow (analyst I.A. Roshchina). Analysis for trace elements was carried out in the Analytical Laboratory of the Institute of Geology of Ore Deposits, Petrography, Mineralogy, and Geochemistry, Moscow (analyst Ya.V. Bychkova). The sample preparation procedure and analysis technique are described in detail by Bychkova et al. (2016). The measurements were carried out using an Element-XR mass spectrometer with inductively coupled plasma. The sample was sprayed into an argon flow in the mass spectrometer and ionized in the inductively coupled plasma. The detection limits were 0.01 ppb for heavy and medium-weight elements and up to 1 ppb for light elements. The measurement error was 1–3 rel.%. The quality of the measurements was controlled by analysis of the standard samples BCR-2 and SG-3.

The diagrams were plotted on LOI-free basis.

RESULTS

Tera–Wasserburg diagrams for the studied zircons are presented in Fig. 4, and the corresponding analytical data are listed in Table 2. Figure 5 shows the results of $^{40}Ar/^{39}Ar$ dating of the biotite extracted from sample 255.01/08.

For zircons from samples 374.03/08 and 384.03/08 (dacitic ignimbrite and trachyrhyolitic lava from the East Berezovaya Formation), the error ellipses follow the discordia line (Fig. 4*a*,*b*). For both samples, the discordia lines intersect the vertical axis at ca. $^{207}Pb/^{206}Pb$ = 0.843; hence, the discordance might result from the minor common lead contamination. The discordia lines cross the concordia at 122.0 ± 2.5 and 119.0 ± 1.5 Ma; both dates correspond to an Aptian age. For sample 384.03/08, the common-lead correction yields a concordant age of 119.5 ± 2.0 Ma, only slightly different from the uncorrected result. The statement about the Aptian pulse of the UMVB activity is confirmed by the ages of detrital zircons from the sequences of the UMVB forearc basin located ~100 km east of the Ubienka uplift (Moiseev, 2015).

Sample 381.03/08 (porphyritic dacite collected within the block composed by the Travka Formation) contains zircons of several age groups. The age of the largest population (six grains) falls in the interval 120–130 Ma. Two zircon crystals display a relatively ancient U–Pb age of 362.6 ± 5.4 and 143.1 ± 2.3 Ma, and four grains yield a U-Pb age between 101 and 87 Ma (Fig. 4*c*). Since the validity of the Tithonian–Berriasian age of the Travka Formation is con-

Table 1. Chemical composition of volcanic rocks of the Uda–Murgal and Okhotsk–Chukotka volcanic belts (basins of the Ubienka and Chineiveem rivers)

Component	Sample									
	383.04/08	380.02/08	380.04/08	381.01/08	381.05/08	373.01/08	373.03/08	374.02/08	374.03/08	376.01/08
	65°29′48″; 170°21′33″*	65°30′05″; 170°20′07″	65°30′03″; 170°20′02″	65°29′49″; 170°20′02″	65°29′43″; 170°20′26″	65°32′10″; 170°18′16″	65°31′59″; 170°18′05″	65°31′46″; 170°18′36″	65°31′45″; 170°18′54″	65°31′31″; 170°19′41″
	1	2	3	4	5	6	7	8	9	10
SiO_2	56.08	47.14	54.35	52.82	50.93	60.38	61.40	61.46	65.05	60.02
TiO_2	0.96	1.16	1.25	0.75	1.16	0.68	0.77	0.77	0.57	0.89
Al_2O_3	19.15	14.83	17.82	18.72	16.93	18.03	18.77	19.28	15.64	17.85
Fe_2O_3	7.42	11.69	7.96	8.89	10.04	3.93	3.78	4.14	3.92	7.23
MnO	0.22	0.15	0.22	0.22	0.16	0.12	0.11	0.11	0.08	0.22
MgO	2.84	7.96	2.90	3.33	3.32	1.84	1.20	1.30	1.65	1.85
CaO	2.21	7.41	5.05	4.23	5.66	2.13	2.30	2.01	3.01	1.46
Na_2O	5.54	2.14	4.49	5.48	3.43	3.81	4.43	5.06	3.48	4.88
K_2O	2.17	1.11	1.68	0.99	2.42	4.57	3.95	3.31	3.53	2.59
P_2O_5	0.60	0.36	0.66	0.71	0.35	0.23	0.20	0.21	0.15	0.27
LOI	2.52	5.65	3.11	3.48	5.22	3.74	2.66	2.06	2.46	2.41
Total	99.71	99.60	99.49	99.63	99.62	99.45	99.57	99.71	99.55	99.68
Cs	0.58	1.45	0.96	0.17	2.75	3.99	1.75	0.97	4.94	0.18
Rb	27.2	16.7	22.1	12.3	51.8	90.3	76.2	37.7	67.6	30.8
Ba	716	904	1108	435	1536	1161	934	968	980	558
Th	7.16	6.22	7.56	4.29	8.56	25.31	24.02	24.45	18.89	7.86
U	0.97	0.91	1.02	0.53	1.22	3.58	3.43	3.27	2.36	0.99
Nb	13.75	3.25	11.44	6.81	4.57	7.92	7.98	7.99	6.03	19.54
Ta	0.95	0.36	0.87	0.53	0.38	0.80	0.75	0.70	0.54	1.38
La	21.2	13.7	20.2	14.9	16.8	26.6	27.9	26.6	23.9	27.7
Ce	45.3	30.6	44.6	32.9	36.1	56.3	57.9	54.7	45.8	58.5
Pb	9.35	6.90	5.95	4.93	5.10	17.19	17.83	14.55	13.13	6.72
Pr	5.86	4.34	6.07	4.50	4.91	7.22	7.25	6.74	5.51	7.39
Sr	539	658	866	572	672	554	386	369	389	323
Nd	25.0	19.3	26.1	19.9	21.3	29.0	28.9	26.8	21.3	29.9
Zr	186	87.9	177	94.9	124	294	299	303	87.3	313
Hf	4.36	2.37	4.25	2.51	3.28	7.41	7.43	7.48	2.83	7.00
Sm	5.41	4.56	6.13	4.39	4.92	5.96	6.05	5.53	4.19	6.55
Eu	1.93	1.65	2.03	1.52	1.84	1.75	1.79	1.78	1.28	2.07
Gd	5.24	4.36	6.12	4.17	4.67	5.69	5.73	5.37	4.01	6.44
Tb	0.85	0.67	1.02	0.69	0.75	0.89	0.91	0.87	0.61	1.10
Dy	4.73	3.57	5.59	3.79	4.08	4.90	5.08	4.88	3.31	6.29
Y	26.6	18.2	30.3	20.3	21.7	27.6	28.8	28.3	18.0	36.3
Ho	0.98	0.72	1.18	0.77	0.84	1.03	1.07	1.04	0.68	1.34
Er	3.03	2.09	3.48	2.32	2.47	3.17	3.33	3.28	2.03	4.16
Tm	0.45	0.28	0.50	0.33	0.35	0.47	0.50	0.49	0.30	0.63
Yb	3.08	1.88	3.40	2.21	2.34	3.27	3.46	3.44	2.05	4.38
Lu	0.48	0.28	0.51	0.33	0.34	0.51	0.54	0.54	0.31	0.68

(*continued on next page*)

Table 1 (*continued*)

Component	Sample									
	376.02/08	384.03/08	377.01/08	378.01/08	379.01/08	276.02/08	283.01/08	284.01/08	304.01/08	315.01/08
	65°31′24″; 170°19′47″	65°29′49″; 170°22′17″	65°31′11″; 170°19′47″	65°30′44″; 170°19′37″	65°30′30″; 170°19′45″	65°39′10″; 170°11′22″	65°39′09″; 170°09′59″	65°39′06″; 170°11′21″	65°39′31″; 170°13′29″	65°39′27″; 170°18′33″
	11	12	13	14	15	16	17	18	19	20
SiO_2	52.89	68.92	47.42	48.01	45.89	54.02	48.22	56.19	51.19	74.45
TiO_2	1.39	0.37	1.45	1.91	0.99	0.80	0.84	0.92	0.67	0.13
Al_2O_3	16.00	16.26	20.63	18.15	19.66	19.55	20.08	17.79	21.36	14.32
Fe_2O_3	11.47	1.81	9.34	11.85	9.09	8.05	10.36	8.19	8.37	0.99
MnO	0.23	0.05	0.16	0.31	0.14	0.18	0.19	0.18	0.15	0.09
MgO	3.91	0.71	3.52	3.92	4.15	2.45	4.28	0.91	3.12	0.12
CaO	4.93	0.44	10.04	7.60	9.64	6.84	10.16	4.76	9.53	0.58
Na_2O	3.76	4.72	3.47	4.21	2.47	4.25	2.95	4.49	3.61	3.20
K_2O	1.46	5.55	1.03	0.84	0.92	0.39	0.13	1.38	0.37	4.19
P_2O_5	0.38	0.11	0.41	0.47	0.25	0.37	0.37	0.44	0.24	0.03
LOI	3.38	0.84	2.20	2.39	6.52	2.95	2.32	4.48	1.34	1.60
Total	99.80	99.78	99.67	99.66	99.72	99.85	99.90	99.73	99.95	99.70
Cs	0.16	0.39	0.10	0.12	0.50	1.05	0.73	1.34	0.57	1.20
Rb	26.2	100.4	13.2	8.0	13.1	5.6	1.1	16.9	3.5	73.9
Ba	319	882	465	513	292	303	176	580	227	1241
Th	4.88	23.25	4.58	3.89	4.46	1.18	0.52	1.86	0.56	6.06
U	0.62	2.70	0.59	0.55	0.46	0.42	0.19	0.68	0.21	1.63
Nb	4.51	5.43	4.94	6.84	1.94	3.30	2.52	5.93	1.83	4.71
Ta	0.48	0.52	0.51	0.58	0.30	0.66	0.51	0.53	0.37	0.43
La	12.1	18.9	11.4	12.7	8.6	11.8	7.2	17.3	7.2	19.3
Ce	28.0	37.0	25.3	29.3	19.3	26.9	17.2	39.6	17.6	33.9
Pb	3.49	14.65	4.49	5.52	7.55	6.90	2.81	14.08	3.85	10.63
Pr	3.95	4.34	3.57	4.28	2.78	3.90	2.40	5.79	2.48	3.39
Sr	277	156	709	621	713	744	643	306	755	71
Nd	18.2	15.9	16.4	20.3	12.9	17.6	11.3	25.4	11.3	11.2
Zr	134	95.6	80.1	109	49.9	82.2	56.0	160.7	55.0	81.5
Hf	3.62	2.97	2.17	2.82	1.46	2.42	1.59	4.23	1.40	2.29
Sm	4.75	3.13	4.03	5.29	3.13	4.30	2.90	6.21	2.72	1.86
Eu	1.47	0.94	1.44	1.89	1.11	1.45	1.03	1.64	0.95	0.26
Gd	4.98	2.92	4.03	5.31	2.88	4.00	2.80	5.63	2.49	1.19
Tb	0.88	0.46	0.67	0.90	0.45	0.69	0.50	0.97	0.43	0.26
Dy	5.32	2.52	3.73	5.18	2.32	4.19	3.12	5.63	2.53	1.42
Y	28.7	15.0	19.6	27.4	11.2	22.1	17.1	29.4	13.7	8.90
Ho	1.11	0.53	0.78	1.07	0.46	0.84	0.64	1.14	0.51	0.30
Er	3.27	1.68	2.26	3.09	1.31	2.36	1.85	3.14	1.42	0.91
Tm	0.47	0.26	0.32	0.43	0.17	0.34	0.27	0.46	0.21	0.15
Yb	3.08	1.78	2.08	2.82	1.09	2.28	1.82	3.04	1.36	1.10
Lu	0.47	0.27	0.31	0.41	0.15	0.34	0.27	0.45	0.20	0.17

(*continued on next page*)

Table 1 (*continued*)

Component	Sample									
	316.01/08	365.02/08	365.03/08	366.02/08	367.01/08	255.01/08	256.01/08	380-67/02	90-446/02	88-4824/02
	65°39′39″; 170°18′51″	65°36′05″; 170°08′50″	65°36′03″; 170°08′52″	65°35′55″; 170°08′48″	65°35′47″; 170°09′09″	65°50′33″; 171°21′24″	65°50′23″; 171°22′02″	66°08′01″; 171°35′12″	66°11′30″; 171°50′36″	66°13′28″; 171°49′20″
	21	22	23	24	25	26	27	28	29	30
SiO_2	53.26	50.83	54.90	74.72	66.89	66.35	66.75	64.14	71.61	71.57
TiO_2	0.92	0.79	0.65	0.12	0.71	0.47	0.51	0.52	0.24	0.24
Al_2O_3	17.66	21.60	19.94	14.22	16.46	16.32	14.75	15.37	13.42	12.89
Fe_2O_3	9.08	8.20	7.29	1.09	3.91	4.36	4.98	5.12	1.92	1.88
MnO	0.15	0.15	0.15	0.03	0.13	0.06	0.08	0.07	0.03	0.02
MgO	4.04	3.00	2.82	0.11	0.49	0.76	0.59	1.98	0.30	0.26
CaO	8.70	8.95	8.06	0.69	2.35	3.91	4.71	4.51	1.21	0.98
Na_2O	2.69	3.63	3.55	3.65	4.53	2.76	3.62	2.83	2.15	2.53
K_2O	1.14	0.11	0.80	3.83	2.92	3.90	2.90	2.95	6.40	5.19
P_2O_5	0.29	0.25	0.24	0.03	0.16	0.14	0.12	0.15	0.05	0.04
LOI	1.99	1.94	1.58	1.08	1.26	0.69	0.95	1.80	1.35	3.41
Total	99.91	99.44	99.98	99.57	99.81	99.02	99.96	99.44	98.68	99.02
Cs	0.49	N.a.	N.a.	0.71	0.29	2.88	4.31	3.71	3.45	2.13
Rb	12.6	0.9	9.1	58.4	33.8	112.6	100.6	96.0	209.4	176.8
Ba	548	243	431	1208	931	685	647	634	697	698
Th	2.61	0.85	1.03	6.70	2.42	12.04	11.11	10.85	18.68	17.09
U	0.97	0.23	0.40	1.72	0.88	1.92	3.19	3.23	3.86	4.75
Nb	3.70	2.99	2.90	5.17	9.91	7.75	7.87	7.61	7.00	6.84
Ta	0.29	0.27	0.33	0.49	0.61	0.55	0.53	0.53	0.74	0.68
La	13.8	9.8	9.9	26.0	18.1	25.7	27.8	25.8	31.3	33.0
Ce	31.7	23.0	22.9	33.5	42.0	50.0	56.4	54.2	61.6	64.0
Pb	7.87	5.03	3.92	24.37	10.22	16.20	17.00	14.84	20.45	20.30
Pr	4.27	3.20	3.04	4.76	5.58	5.96	6.81	6.23	6.43	6.67
Sr	552	654	575	145	257	297	333	296	181	158
Nd	18.3	14.1	13.4	15.3	23.2	22.4	25.8	24.0	21.8	22.3
Zr	125	75.7	74.2	84.7	185	109	114	105	144	126
Hf	3.27	1.92	1.64	2.41	4.99	3.54	3.62	3.37	4.34	3.83
Sm	4.21	3.48	3.17	2.55	5.46	4.33	4.98	4.61	3.67	3.70
Eu	1.08	1.16	1.04	0.33	1.40	0.81	0.88	0.82	0.68	0.66
Gd	3.97	3.20	2.92	1.55	4.96	3.96	4.75	4.53	2.92	3.01
Tb	0.69	0.59	0.51	0.34	0.95	0.59	0.71	0.68	0.42	0.45
Dy	4.08	3.48	3.17	1.88	5.78	3.54	4.15	4.00	2.35	2.62
Y	22.7	19.1	16.8	9.9	33.4	19.0	23.2	23.5	15.8	18.9
Ho	0.84	0.72	0.65	0.37	1.18	0.72	0.85	0.82	0.50	0.56
Er	2.35	2.04	1.83	1.10	3.52	2.16	2.56	2.49	1.38	1.64
Tm	0.34	0.31	0.26	0.18	0.54	0.32	0.38	0.36	0.24	0.28
Yb	2.25	1.86	1.68	1.30	3.70	2.24	2.57	2.42	1.76	2.14
Lu	0.33	0.28	0.23	0.19	0.57	0.34	0.39	0.37	0.26	0.32

Note. Major-oxide contents are in wt.%, and trace-element contents are in ppm. Major-oxide analysis was carried out by XRF at the Institute of Geochemistry and Analytical Chemistry, Moscow (analyst I.A. Roshchina), and trace-element analysis was performed by ICP MS at the Institute of Geology of Ore Deposits, Petrography, Mineralogy, and Geochemistry, Moscow (analyst Ya.V. Bychkova); N.a., not analyzed. 1–15, UMVB rocks: 1–5, Travka Formation, 6–15, East Berezovaya Formation; 16–30, OCVB rocks: 16–19, Ubienka Formation, 20–25, Kavral'yanskaya Formation, 26, 27, Vapanai Formation, middle course of the Chineiveem River; 28–30, Vapanai and Emuneret formations, upper course of the Chineiveem River.
* Geographic coordinates (N, E).

Table 2. Results of U–Pb zircon dating

Analysis	$^{206}Pb_c$, %	U	Th	Th/U	$^{238}U/^{206}Pb \pm \%$	$^{207}Pb/^{206}Pb \pm \%$	Age, ± 1σ, Ma
		ppm					
Sample 374.03/08 (dacitic ignimbrite from the East Berezovaya Formation); 65°31′45″ N, 170°18′54″ E							
1.1	7.06	95	77	0.84	47.0 ± 3.3	0.1337 ± 7.1	126.2 ± 7.9
2.1	9.62	106	83	0.82	46.5 ± 2.7	0.1400 ± 11	124.1 ± 8.3
3.1	10.08	96	51	0.55	44.5 ± 2.8	0.1520 ± 12	128.8 ± 9.1
4.1	11.14	93	71	0.78	45.6 ± 2.9	0.1548 ± 5.7	124.2 ± 8.6
5.1	15.02	71	42	0.61	42.5 ± 3.2	0.2080 ± 7.9	127.0 ± 12
6.1	13.49	104	79	0.79	43.0 ± 2.7	0.1723 ± 4.6	128.2 ± 9.6
7.1	7.39	139	91	0.68	44.5 ± 2.5	0.1320 ± 15	132.7 ± 6.9
8.1	9.46	109	56	0.53	47.0 ± 2.7	0.1310 ± 9.5	122.8 ± 8.1
9.1	6.50	166	92	0.57	48.0 ± 2.3	0.1110 ± 12	124.2 ± 5.8
10.1	8.58	123	81	0.68	48.7 ± 2.6	0.1271 ± 5.4	119.7 ± 7.2
Sample 384.03/08 (trachyrhyolitic lava from the East Berezovaya Formation); 65°29′49″ N, 170°22′17″ E							
1.1	2.54	229	125	0.57	52.3 ± 1.9	0.062 ± 5.2	119.1 ± 2.7
2.1	1.77	622	934	1.55	52.9 ± 1.4	0.0565 ± 3.3	118.7 ± 2.2
3.1	4.44	145	83	0.59	49.7 ± 2.3	0.1001 ± 9.1	122.7 ± 4.3
4.1	1.67	327	126	0.40	51.7 ± 2.1	0.0613 ± 4.7	121.4 ± 2.8
5.1	2.67	157	85	0.56	50.8 ± 2.3	0.0835 ± 5.7	122.2 ± 4.3
6.1	4.73	206	182	0.92	50.4 ± 2.1	0.0959 ± 6.2	120.6 ± 3.9
7.1	2.66	180	115	0.66	52.2 ± 2.2	0.0861 ± 9.1	119.0 ± 3.3
8.1	2.69	286	244	0.88	53.4 ± 1.9	0.0839 ± 10	116.4 ± 3.3
9.1	4.32	236	141	0.62	52.1 ± 2.0	0.0906 ± 5.7	117.4 ± 2.8
10.1	1.62	319	295	0.96	52.3 ± 1.8	0.0705 ± 4.1	120.2 ± 2.8
Sample 381.03/08 (subvolcanic (?) dacite from the block composed of the Travka Formation); 65°29′47″ N, 170°20′08″ E							
4.2	3.87	433	185	0.44	71.1 ± 1.9	0.0904 ± 11	86.6 ± 2.6
4.1	3.68	405	181	0.46	68.4 ± 1.8	0.0897 ± 10	90.2 ± 2.4
5.1	6.59	227	114	0.52	58.7 ± 2.2	0.1170 ± 15	101.6 ± 4.2
5.2	10.03	178	84	0.49	57.1 ± 2.5	0.1307 ± 7.6	100.7 ± 5.6
7.1	4.29	281	276	1.01	51.1 ± 2.0	0.0990 ± 12	119.6 ± 3.9
3.1	5.13	225	139	0.64	50.6 ± 2.1	0.0980 ± 15	119.7 ± 4.5
2.1	3.59	206	115	0.58	48.9 ± 2.2	0.0947 ± 8.2	125.8 ± 3.8
6.1	10.71	99	53	0.56	44.2 ± 2.9	0.1657 ± 5.5	128.9 ± 9.7
7.2	4.50	399	659	1.71	48.9 ± 1.8	0.0896 ± 6.8	124.6 ± 3.4
6.2	14.64	98	53	0.56	41.9 ± 2.9	0.1888 ± 5.1	130.0 ± 12
1.1	1.74	603	339	0.58	43.8 ± 1.5	0.0646 ± 6.1	143.1 ± 2.3
8.1	1.02	355	227	0.66	17.1 ± 1.4	0.0610 ± 4.2	362.6 ± 5.4

Note. Analysis was carried out using a SHRIMP-II ion microprobe at the Center of Isotope Research of the Russian Geological Research Institute, St. Petersburg (analyst A.N. Larionov). The ages of individual grains were corrected for common lead using measured ^{204}Pb.

firmed paleontologically (Malysheva et al., 2012), the studied sample might be either OCVB-related rock (presumably of Coniacian age) carrying abundant material trapped from older complexes or a rock of an uncertain age with a disturbed U–Pb system.

The $^{40}Ar/^{39}Ar$ plateau age of biotite from sample 255.01/08 (dacite lava from the Vapanai Formation) is 88.7 ± 1.2 Ma (97.4% of released ^{39}Ar), which approximately corresponds to the Turonian/Coniacian boundary. The integrated $^{40}Ar/^{39}Ar$ age of the sample is 89.7 ± 1.3 Ma. This date contradicts the earlier reported Santonian age of the Vapanai Formation and the Coniacian–Campanian age of the Pastbishchnaya Formation unconformably overlain by the Vapanai Formation (Malysheva et al., 2012).

The $^{40}Ar/^{39}Ar$ age spectrum (Fig. 5) and the distribution of error ellipses in the Tera–Wasserburg diagrams (Fig. 4) do not display any significant disturbance of the isotope systems of the studied samples (except for sample 381.03/08).

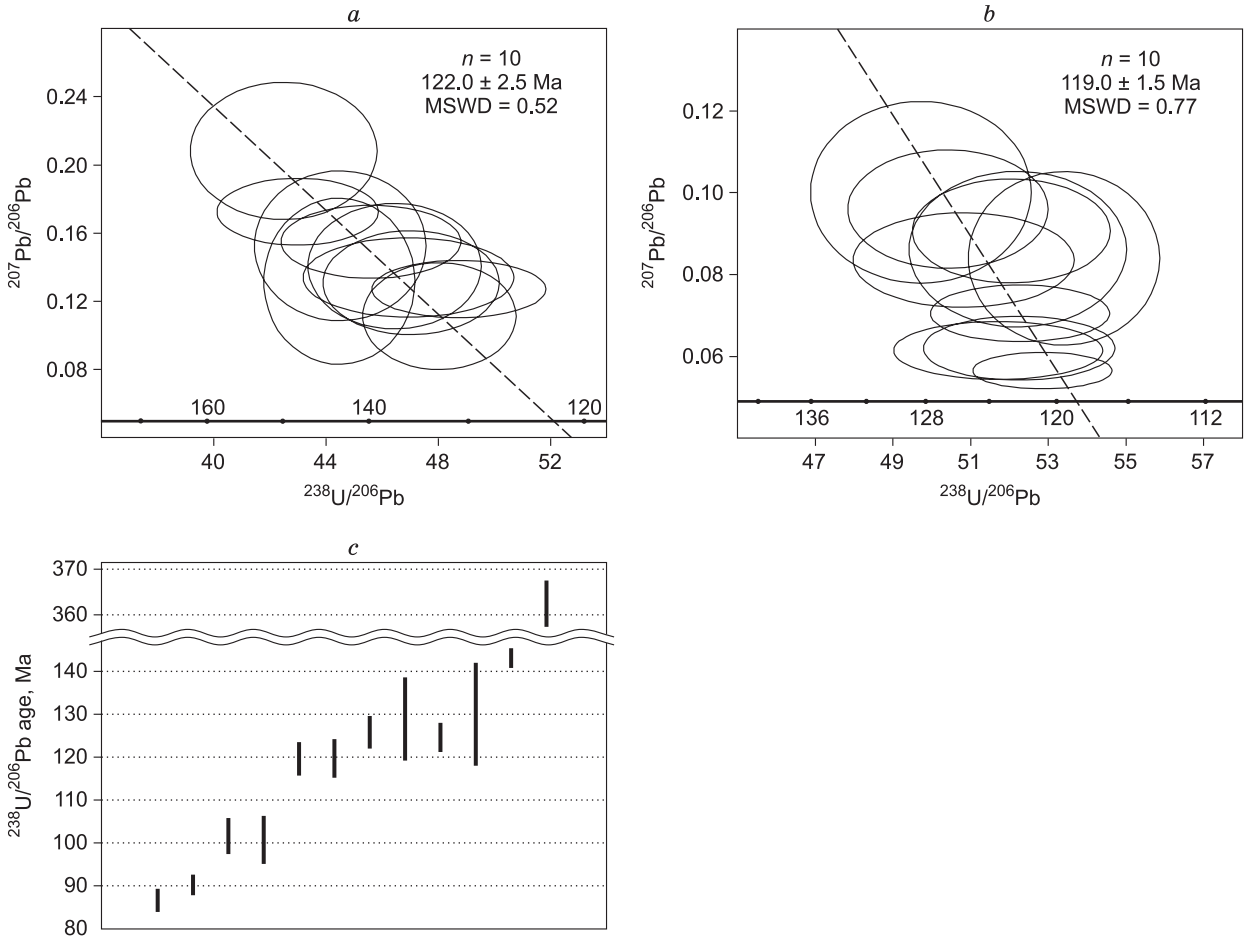

Fig. 4. Tera–Wasserburg diagrams for zircons from samples 374.03/08 (*a*) and 384.03/08 (*b*); the $^{238}U/^{206}Pb$ age of individual zircon grains from sample 381.03/08 (after correction for common lead, based on the measured ^{204}Pb; the height of segments corresponds to 2σ) (*c*).

Taking into account the weak hydrothermal alteration of the rock samples, we conclude that the dating results directly indicate the age of the corresponding magmatic events, which suggest that the East Berezovaya Formation belongs to the UMVB rather than to the OCVB.

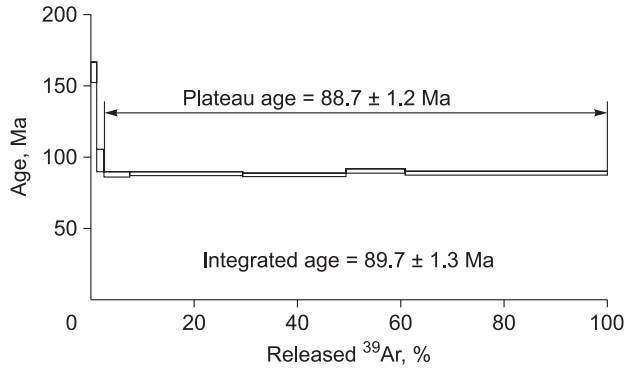

Fig. 5. $^{40}Ar/^{39}Ar$ release spectra for biotite from sample 255.01/08.

GEOCHEMISTRY OF VOLCANICS OF THE UDA–MURGAL AND OKHOTSK–CHUKOTKA BELTS

The results of chemical analyses of the UMVB and OCVB volcanic rocks are presented in Table 2 and in Figs. 6–12. The diagrams also include data for two rock samples from the Koekvun'(?) Formation (OCVB), collected in the Chineiveem River basin, 70 km northeast of the Ubienka uplift (Tikhomirov et al., 2016).

In addition, we used the results of 332 major-element analyses from geological reports of the 1960–1980s (Lobunets and Kuznetsova, 1977; Trunov, 1977) for comparison. The historical data were kindly provided by our colleagues from the Georegion Federal State Unitary Geological Enterprise (Anadyr'). Most of the above analyses were carried out by the wet chemistry method in the Central Laboratory of the Sevvostgeologiya Production Geological Association (Magadan). The set of major-element analysis data used in this paper is representative for the northern part of the Murgal segment of the UMVB (112 analyses) and the frontal zone of the Anadyr' segment of the OCVB (256 analyses).

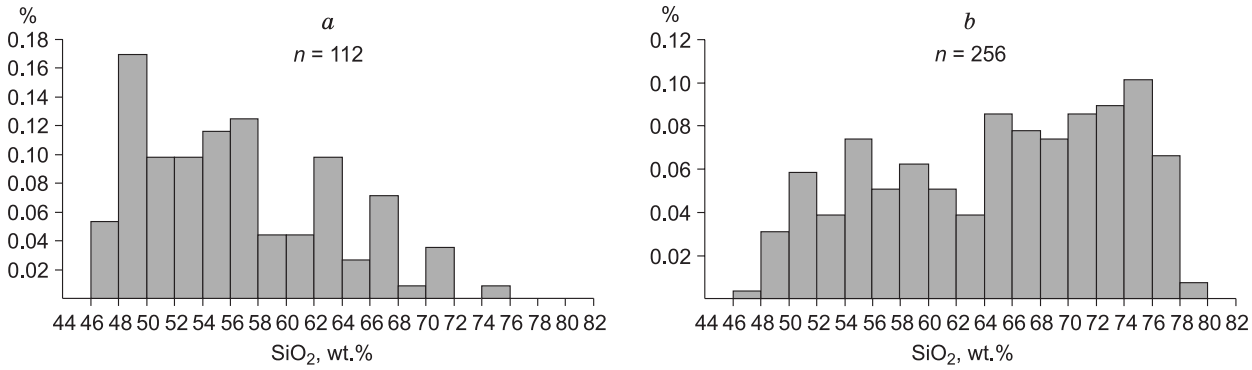

Fig. 6. Histograms of SiO_2 contents in the UMVB (*a*) and OCVB (*b*) rocks within the area shown in Fig. 1.

Major oxides. The UMVB and OCVB volcanics form a continuous series from basalts to rhyolites. Basalts and andesites prevail in the UMVB complexes, whereas dacites and rhyolites are predominant in the OCVB (Fig. 6). Within the area shown in Fig. 1, the UMVB rocks display somewhat lower average contents of P_2O_5 and K_2O and, correspondingly, lower $K_2O/(K_2O + Na_2O)$ ratios as compared with the OCVB volcanics. The $K_2O + Na_2O$ contents are nearly the same in the UMVB and OCVB rocks (Fig. 7*a*, *h–j*). The correlation between SiO_2 and other major oxides is typical of most of differentiated magmatic series. With increasing silica content, the K_2O content increases, whereas the TiO_2, Al_2O_3, Fe_2O_3, MgO, and CaO contents decrease. The Na_2O content tends to increase at SiO_2 = 47–57% and slowly decreases or remains constant at higher silica contents (see Fig. 7*g*). The proportions of K, Na, Fe, and Mg oxide contents (Fig. 8) suggest that the studied complexes are dominated by derivates of calc-alkaline series. The estimated portion of the tholeiitic-series rocks is ca. 10% for the OCVB and 30% for the UMVB.

The UMVB rocks sampled in the Ubienka River basin reveal higher alkaline-metal contents than OCVB rocks sampled in the same area. In the TAS diagram, the greater part of the UMVB analyses plots in the field of moderately alkaline rocks, whereas the OCVB volcanics fall in the field of normal alkalinity rocks (Fig. 7*a*).

Among the UMVB rocks, the Travka Formation volcanics are less differentiated (from basalts to trachyandesites), whereas the East Berezovaya Formation contains abundant silicic rocks, and its composition is bimodal, with basalts and trachydacites being the most ubiquitous rocks (Fig. 7*a*). The studied basalts of both the Travka and East Berezovaya Formations are relatively enriched in TiO_2 (1–2% against 0.7–0.9% in the OCVB basalts) and K_2O (0.9–1.2% against 0.1–0.4%). Thus, within the large structures (e.g., segments of the volcanic belts), the UMVB complexes are depleted in incompatible elements as compared with the OCVB rocks, but within the Ubienka uplift and in its immediate vicinity the UMVB rocks are, on the contrary, relatively enriched.

Trace elements. Both the OCVB and UMVB rocks display features typical of subduction zone magmas, e.g., depletion in Ta and Nb, enrichment in Pb, and high LILE/HFSE and LILE/REE ratios (Fig. 9). The silicic and intermediate/mafic volcanics show patterns of incompatible lithophile elements similar to each other and the patterns of IAB (Shibata and Nakamura, 1997) and the continental upper crust (Rudnick and Gao, 2004). The basalts and andesites from the Ubienka River basin show a geochemical affinity with mafic and intermediate volcanics from other parts of the Anadyr' segment of the OCVB (Tikhomirov et al., 2016). On this background, the rocks of Ubienka and Kavral'yanskaya Formations look anomalous, being substantially depleted in LILE (Fig. 9*c*).

The studied rock samples are moderately enriched in LREE relative to HREE (Fig. 10). The La/Yb ratio varies from 4 to 14 in intermediate and mafic rocks, and from 5 to 20 in silicic rocks. Significant Eu depletion is observed only in the OCVB silicic volcanics (Eu/Eu* = 0.51–0.82); the other samples show weak Eu anomalies (Eu/Eu* = 0.81–1.17).

The incompatible-element abundances increase with the SiO_2 content (Fig. 11*a*, *b*). The ratios of incompatible elements with similar partition coefficients (e.g., Zr/Hf and Ba/Th) do not reveal any significant correlation with SiO_2 (Fig. 11*c*, *d*). In most of the diagrams depicting correlations between such ratios (Fig. 12*a*, *b*), the studied rocks form three negligibly overlapping clusters: (1) the UMVB volcanics (without separation of the rocks of the Travka and East Berezovaya Formations); (2) the OCVB volcanics from the periphery of the Ubienka uplift (Ubienka and Kavral'yanskaya Formations); and (3) the OCVB volcanics exposed north of the Ubienka uplift, in the Chineiveem River basin (Vapanai and Emuneret Formations). The following features can be considered distinctive for the above three geochemical groups: The UMVB rocks have high contents of LILE, high Zr/Hf ratios, and low Ba/Th ratios; the OCVB rocks from the basin of the Ubienka River have low contents of LILE, minimum Th/Nb ratios, and relatively high Ba/Th ratios; and the OCVB rocks from the Chineiveem River basin are characterized by high La/Yb, La/Ta, and Nd/Zr ratios (Fig. 12). In the SiO_2–Th diagram, the three geochemical clusters follow three different trend lines (Fig. 11*a*).

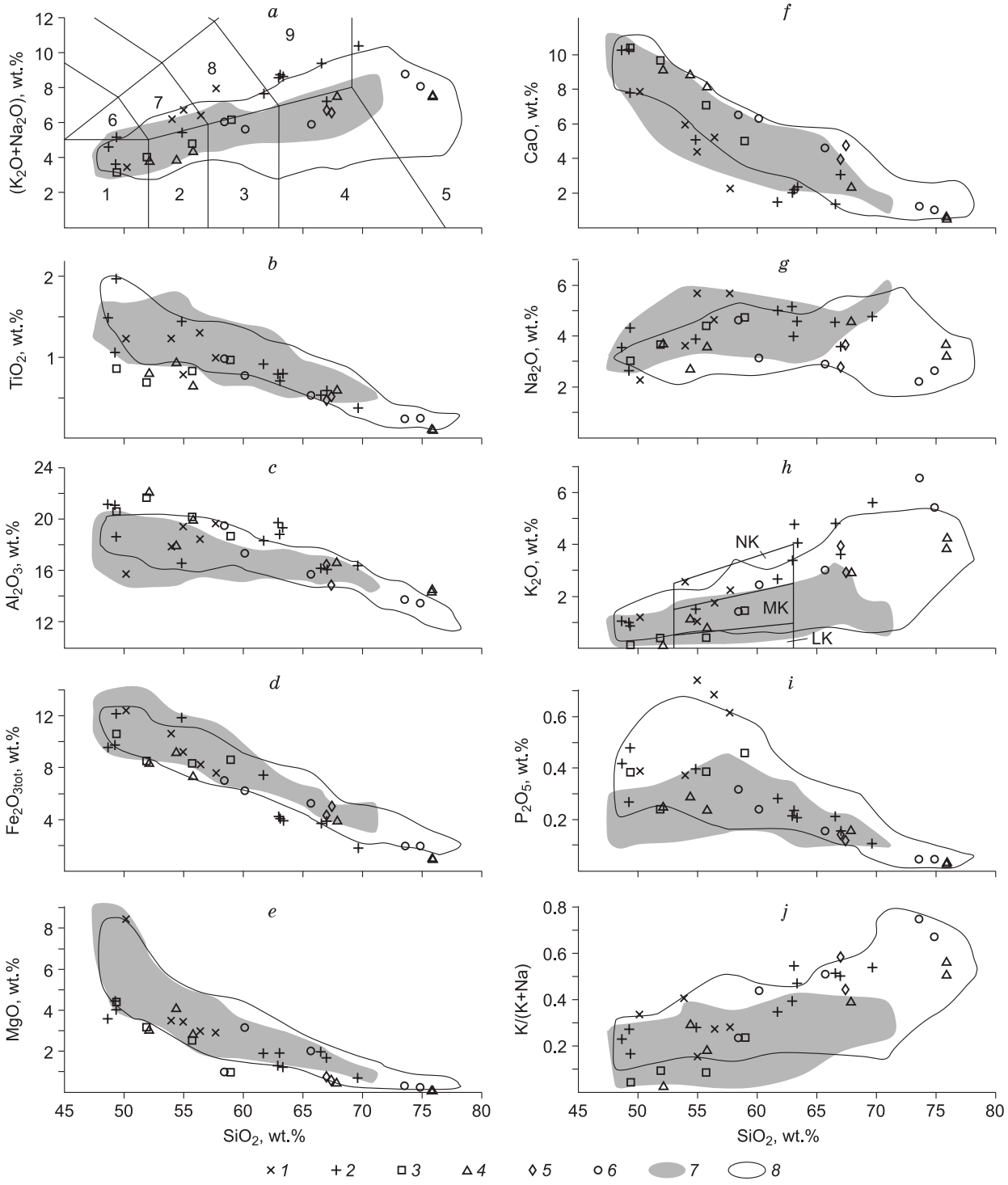

Fig. 7. Major-oxide diagrams for the studied volcanic rocks: *a*, TAS diagram, *b–i*, Harker diagrams, *j*, SiO_2–K/(K + Na) diagram. *1*, *2*, UMVB volcanics: *1*, Travka Formation, *2*, East Berezovaya Formation; *3–6*, OCVB volcanics: *3*, *4*, Ubienka River basin (*3*, Ubienka Formation, *4*, Kavral'yanskaya Formation), *5*, middle course of the Chineiveem River (Vapanai Formation), *6*, upper course of the Chineiveem River (Koekvun'(?), Emuneret, and Vapanai formations); *7*, *8*, compositional fields of volcanic rocks (Trunov, 1977; Lobunets and Kuznetsova, 1977): *7*, UMVB (112 samples), *8*, OCVB (256 samples). Numbers and characters in the diagrams: *a*, after Le Maitre (1989): 1, basalts, 2, basaltic andesites, 3, andesites, 4, dacites, 5, rhyolites and trachyrhyolites, 6, trachybasalts, 7, basaltic trachyandesites, 8, trachyandesites, 9, trachydacites and trachytes; *h*, after Gill (1981): LK, low-K, MK, medium-K, HK, high-K series.

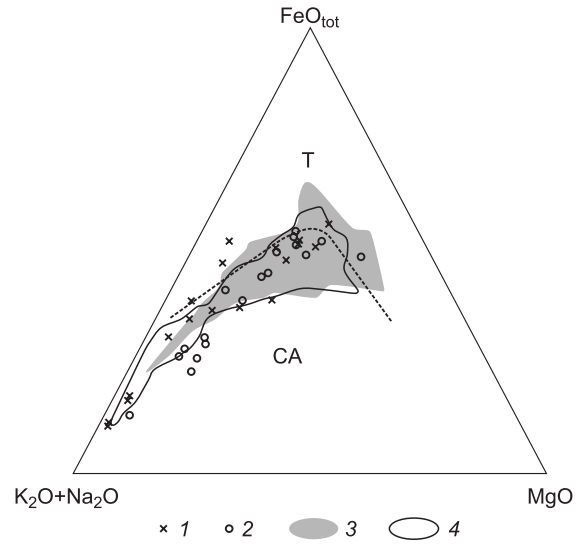

Fig. 8. AFM ((K_2O + Na_2O)–FeO_{tot}–MgO) diagram. *1*, *2*, this study (*1*, UMVB, *2*, OCVB); *3*, *4*, analyses performed in the 1960–1980s (*3*, UMVB, *4*, OCVB). T, tholeiitic series, CA, calc-alkaline series.

DISCUSSION

Considering the above results of field observations, isotopic-age determination, and geochemical data, we propose some corrections to the existing model of the geologic history of northeastern Asia.

TECTONIC EVENTS

In the basins of the Ubienka and Chineiveem Rivers, the late Mesozoic complexes have preserved traces of at least three compressional tectonic events accompanied by folding.

(1) The event that separated the accumulation of the Travka Formation and the East Berezovaya Formation was accompanied by the transition from marine sedimentation and subaqueous volcanic activity to subaerial eruptions. The new U–Pb zircon dates along with the known paleontological age of the Travka Formation constrains the age of this tectonic event to Valanginian–Barremian time. South of the study area, within the area of the Murgal uplift, there are

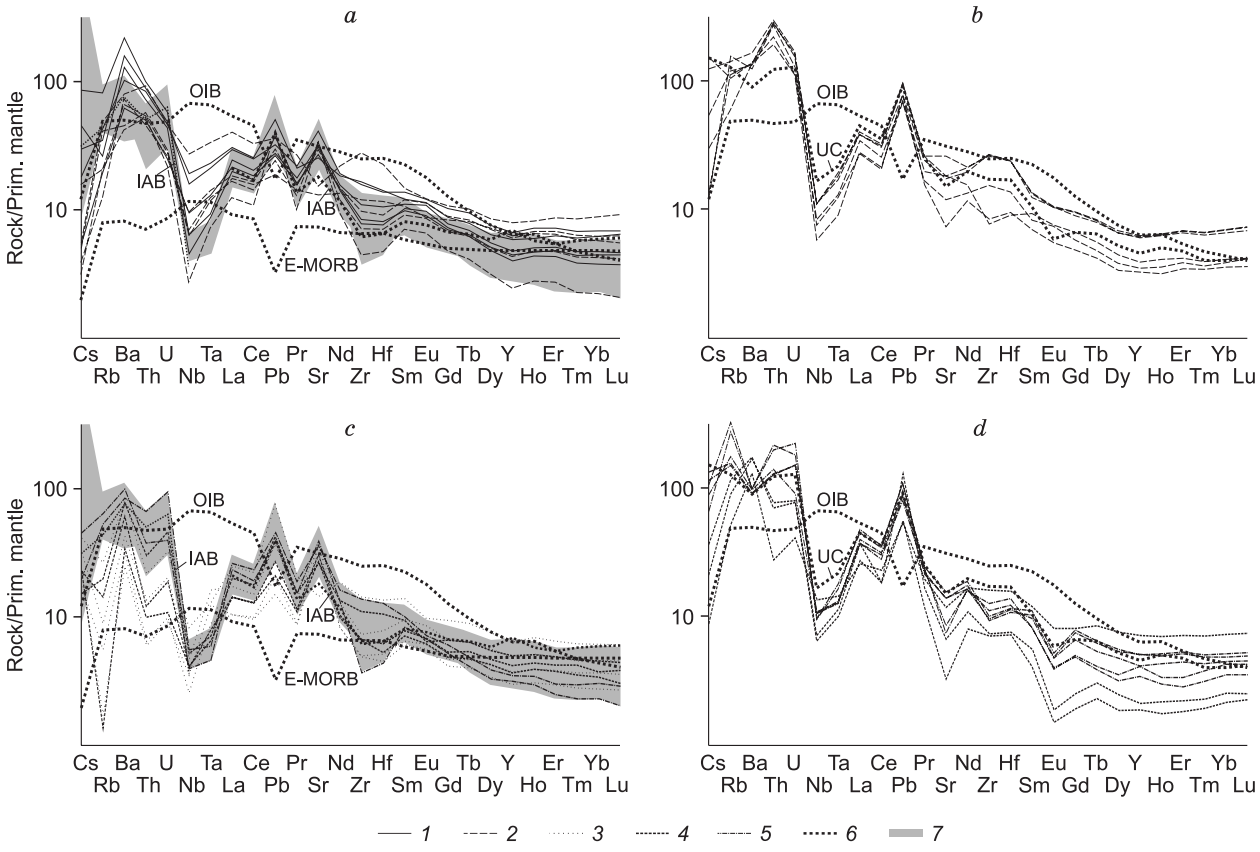

Fig. 9. Primitive mantle-normalized (Sun and McDonough, 1989) spidergrams for the UMVB and OCVB volcanics. *a*, *b*, UMVB (*a*, mafic and intermediate rocks, *b*, silicic rocks); *c*, *d*, OCVB (*c*, mafic and intermediate rocks, *d*, silicic rocks). *1–4*, volcanics of the Ubienka River basin: *1*, Travka Formation, *2*, East Berezovaya Formation, *3*, Ubienka Formation, *4*, Kavral'yanskaya Formation; *5*, volcanics of the Chineiveem River basin (Koekvun'(?), Emuneret, and Vapanai formations); *6*, reference compositions of basalts (OIB and E-MORB (Sun and McDonough, 1989); IAB, average composition of basalts of northeastern Japan (Shibata and Nakamura, 1997); UC, composition of the upper continental crust (Rudnick and Gao, 2004)); *7*, compositional field of volcanics of the Anadyr' segment of the OCVB (Tikhomirov et al., 2016).

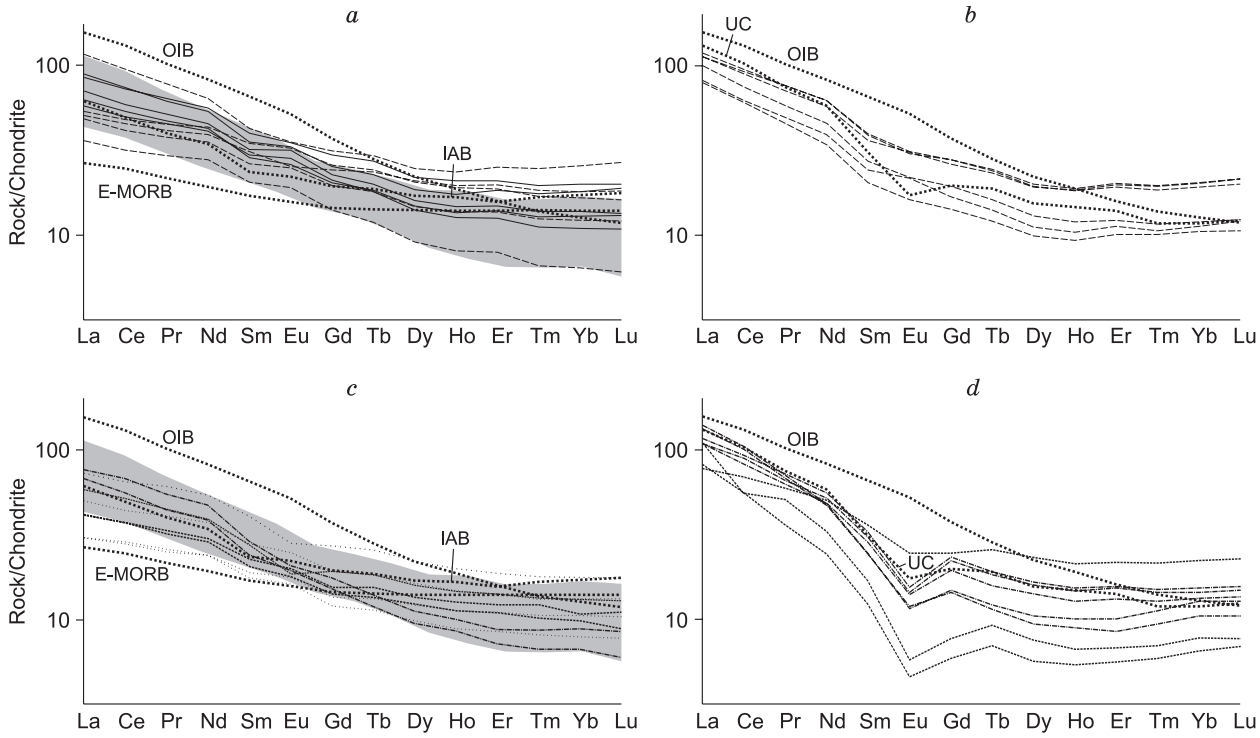

Fig. 10. Chondrite-normalized (Sun and McDonough, 1989) REE patterns of the UMVB and OCVB volcanics. *a*, *b*, UMVB (*a*, mafic and intermediate rocks, *b,* silicic rocks), *c*, *d*, OCVB (*c*, mafic and intermediate rocks, *d*, silicic rocks). Other symbols as in Fig. 9.

Valanginian and Hauterivian volcanic and sedimentary strata, which overlie the Travka Formation with a slight unconformity (Malysheva et al., 2012). Therefore, the age of major tectonic deformations, likely, corresponds to Barremian time (130–125 Ma). The unconformity between Hauterivian and Aptian–Albian strata is observed over a large area, which spreads southwestward to the coast of Penzhina Bay (Lobunets and Kuznetsova, 1977; Makhonina and Bakai, 1979). This tectonic event might also have affected the southwestern segments of the UMVB, because the available $^{40}Ar/^{39}Ar$ and U–Pb dates do not reveal any Hauterivian or Aptian volcanic complexes on the ancient Pacific margin west of the Koni Peninsula.

The pre-Aptian tectonic event was probably caused by the accretion of a block of continental or transitional crust to the margin of the Siberian continent. Since the lithology of the Travka Formation is typical of island arc complexes, we assume that the accreted block was an island arc. Before the Barremian, this block was separated from the continent by a back-arc basin. After the accretion, the volcanic activity resumed in the Andean-type setting. This hypothesis explains the observed pre-Aptian angular unconformity, the transition from marine depositional environments to continental ones, and the significant change in magma composition (see below). The southern segments of the UMVB are superposed on the edge of the Siberian Platform and undoubtedly formed in the regime of an Andean-type margin (Goryachev, 2005). In the Tithonian–Berriasian, the suprasubductional igneous province of the northwestern Pacific might have included both Andean-type and island arc segments, with their gradual northeastward (in present-day coordinates) transition from each other. This kind of transition is observed, for example, for the recent Sunda and Kuril–Kamchatka arcs. A similar model was earlier used in the tectonic reconstructions for the northwestern Pacific (Grantz et al., 2011). As an alternative, we consider the model which implies the existence of a double volcanic belt (island arc and continental arc) within the observed part of the Pacific margin at the time near the Jurassic/Cretaceous boundary. The verification of these models requires more representative structural and geochemical data.

Notably, there are no Aptian U–Pb ages of igneous rocks in the southern part of the UMVB, and all available dates fall into the Tithonian–Hauterivian period (Akinin and Miller, 2011). It is not ruled out that the Aptian volcanics of the Ubienka River basin are related to a local magmatic event that affected only the northeastern part of the belt.

(2) The angular unconformity between the UMVB and OCVB complexes in the Ubienka River basin is similar to or even weaker than the pre-Aptian unconformity within the UMVB complexes. The ages of the strata separated by the unconformity imply that the corresponding compressional event occurred during the time span 119–105 Ma (Aptian–Albian). In a first approximation, this event may be considered a boundary tectonic event between the periods of the UMVB and OCVB formation. However, the granitoids of

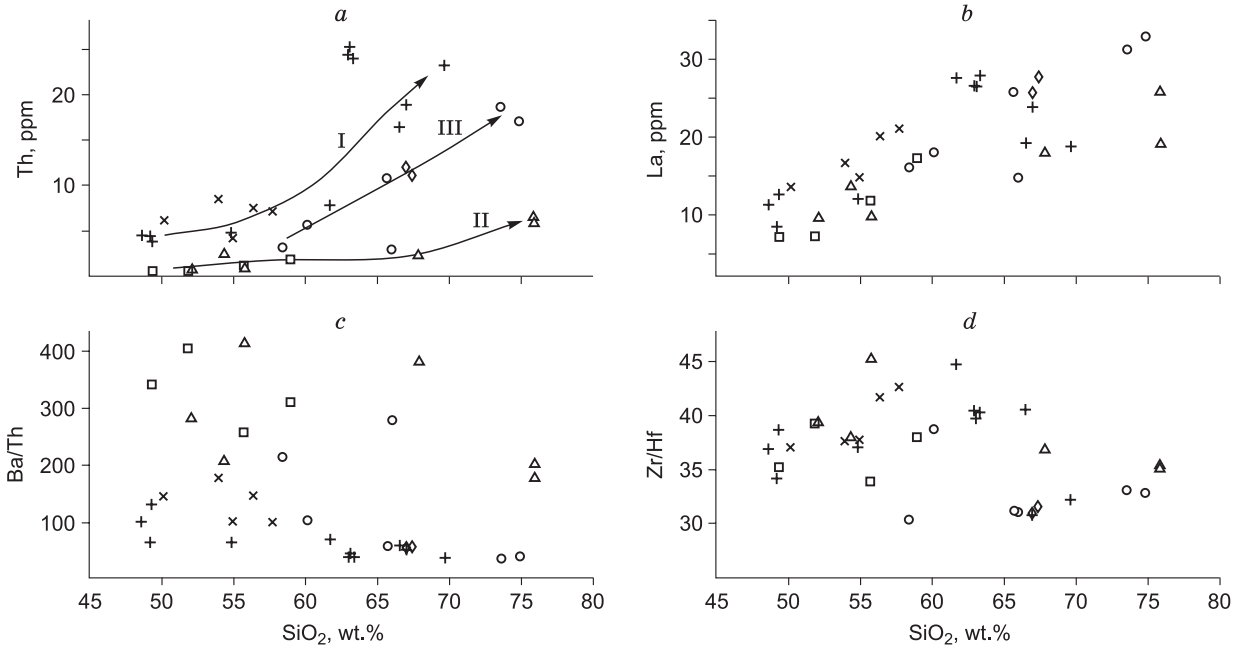

Fig. 11. SiO_2 vs Th, ppm (*a*), La, ppm (*b*), Ba/Th (*c*), and Zr/Hf (*d*) diagrams for the UMVB and OCVB volcanic rocks. *a*, Arrows show the compositional trends of the UMVB rocks (I) and the OCVB rocks collected in the basins of the Ubienka (II) and Chineiveem (III) rivers. Other symbols as in Fig. 7.

the East Taigonos batholith (structurally associated with the UMVB and located 100 km east of the front of the OCVB) yield a U–Pb age of 105–97 Ma (Luchitskaya et al., 2003). Taking into account the virtual absence of significant unconformities within the Late Jurassic and Early Cretaceous complexes of the Taigonos Peninsula (Nekrasov, 1976), we conclude that the activity of some UMVB parts persisted during the Albian, after the OCVB initiation. In this context, the early hypothesis about a single Jurassic through Cretaceous magmatic belt (Ustiev, 1963; Belyi, 1969) gains ground again.

(3) The age of the unconformity at the base of the Vapanai Formation is precisely constrained to the late Turonian (~89 Ma). The absence of distinct folds within the Albian strata of the OCVB rear zone (Belyi, 1977; Tikhomirov et al., 2012) suggests that the corresponding compression was rather weak and caused deformations only in the forearc basin strata. The frontal zone of the Penzhina segment of the OCVB might have been subjected to a stronger compression, because some thrust faults were reported here (Filatova, 1988; Montin, 1992). In the back-arc zone of the OCVB, this event caused a rapid uplift and intense erosion, with the exhumation of large Albian plutons. In the Coniacian–Santonian period, these partially eroded plutons were overlain by volcanics (Tikhomirov, 2018). Approximately at the same time with the late Turonian tectonic event, the magmatic system of the OCVB underwent the following changes:

– The OCVB activity decreased in the Cenomanian; there is a minimum in the isotopic-age histogram for igneous rocks (Akinin and Miller, 2011; Tikhomirov et al., 2012);

– after the Cenomanian relative volcanic calm, the average composition of erupting magmas significantly changed. Andesites dominate in the Albian OCVB strata, and silicic rocks prevail in the Turonian–Campanian strata;

– in the Coniacian–Campanian period, the area of intense volcanism shifted by ~100 km to the east (in present-day coordinates). As a result, the folded sedimentary strata of the OCVB forearc basin were overlain by the undeformed subaerial volcanic sequences.

The across-arc migration of subduction-related volcanism is commonly explained by changes in the slab dip angle (Tatsumi and Eggins, 1995; James and Sacks, 1999). According to the conventional model, the oceanward shift of volcanic loci results from the steepening of the Benioff zone. In such cases, however, the plate adhesion weakens, and compression events become less likely. Therefore, the relation of the late Turonian compression with the accretion of a hypothetical crustal block looks reasonable.

TEMPORAL AND SPATIAL VARIATIONS IN MAGMA COMPOSITION

After the pre-Aptian tectonic event, the subaqueous volcanic activity was changed by the essentially subaerial one. Also, the portion of silicic volcanics significantly increased, and trace-element ratios became more variable (Figs. 7 and 9–12). Compositionally, the UMVB volcanics are typical of ensialic island arcs and Andean-type margins (Wilson, 1989; Frolova and Burikova, 1997).

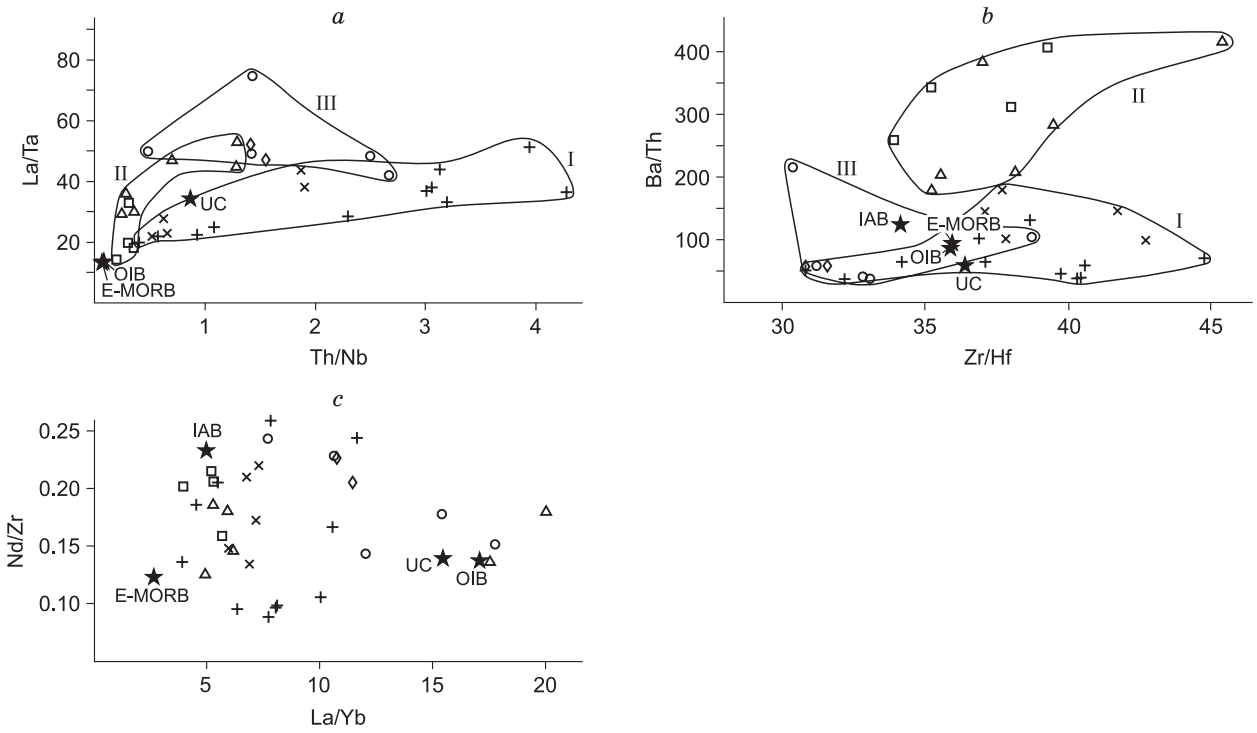

Fig. 12. Th/Nb–La/Ta (*a*), Zr/Hf–Ba/Th (*b*), and La/Yb–Nd/Zr (*c*) diagrams for the UMVB and OCVB volcanic rocks. Asterisks mark the reference compositions of OIB and E-MORB (Sun and McDonough, 1989); *a*, *b*, compositional fields of the UMVB rocks (I) and the OCVB rocks collected in the basins of the Ubienka (II) and Chineiveem (III) rivers. Other symbols as in Figs. 7 and 9.

Within the area shown in Fig. 1, the UMVB and OCVB volcanics are quite similar in term of major element contents. The UMVB rocks have a somewhat lower average silica content and lower K_2O/Na_2O ratios (Fig. 7*j*). This might be due to the progressive heating and melting of the continental crust, which reached a maximum in the Late Cretaceous (Tikhomirov, 2010, 2018). Within the relatively small area of the Ubienka River basin, the compositional difference between the UMVB and OCVB rocks is better pronounced. In addition, the UMVB volcanics here are relatively enriched (Figs. 7 and 9–12) as compared with both the neighboring OCVB sequences and the exposed UMVB rocks in the south, within the Murgal block (Fig. 7). This fact is not consistent with the hypothesis of the gradual thinning of the UMVB crust from south to north (Morozov, 2001; Grantz et al., 2011), because the eruptions of relatively enriched magmas in subduction-related provinces are commonly confined to areas with a relatively thick continental crust (Wilson, 1989; Frolova and Burikova, 1997). This problem requires a detailed geochemical study of both the UMVB and the Late Jurassic–Early Cretaceous igneous complexes of the Chukotka block exposed north of the study area.

Within the studied fragment of the OCVB, some signs of a geochemical zonation are also observed, both along and across the strike of the volcanic belt. The rocks of the frontal zone of the Anadyr' segment of the OCVB (Ubienka and Kavral'yanskaya formations) are depleted in LILE relative to the volcanics of the back-arc zone of the same segment (Fig. 9*c*). This kind of zonation is typical of many subduction-related volcanic belts (Wilson, 1989; Tatsumi and Eggins, 1995; Frolova and Burikova, 1997) but, in the case of the OCVB, the across-arc zonation was earlier supported by major element data only (Kotlyar et al., 1981; Filatova, 1988). Within the neighboring Central Chukotka segment of the OCVB, the across-arc zonation has not been detected, probably because of a significant contamination of mantle magmas with crustal material (Tikhomirov et al., 2016).

Along the strike of the studied OCVB fragment, the incompatible element contents in magmas tend to increase northward (Figs. 9 and 11). There are also systematic changes in trace-element ratios (La/Yb, Th/Nb, Zr/Hf, and Nd/Zr; Fig. 12). The thickness and the age of the continental crust both increase in the same direction. The basement of the Anadyr' segment of the OCVB comprises a collage of Paleozoic–Mesozoic terranes of the Oloi and South Anyui zones (mainly of island arc origin), whereas the Central Chukotka segment overprints the Chukotka block with a Precambrian basement (Miller et al., 2006). The obtained results are consistent with the published data on the along-strike geochemical zonation of the OCVB (Kotlyar et al., 1981; Filatova, 1988; Akinin and Miller, 2011; Tikhomirov et al., 2016). The inferred hierarchy of the factors that control this zonation (the composition of mantle sources and crustal contaminants, the contribution of each source, etc.) cannot yet be clearly deduced from the available data. Some isotopic studies suggest that the composition of the subcon-

tinental lithospheric mantle plays a major role in the large-scale geochemical zonation of the OCVB (Tikhomirov et al., 2016; Tikhomirov, 2018).

CONCLUSIONS

(1) The unconformity between the UMVB and OCVB complexes is not expressed stronger than the internal unconformities of these volcanic belts. Taking into account the evidence for the temporal overlap between the UMVB and OCVB complexes, the separation of the two volcanic belts might be debatable.

(2) The observed segment of the continent–ocean transition zone evolved in the ensialic island arc setting during the Late Jurassic and Berriasian. After the accretion of the island arc (which probably occurred in the Barremian time), volcanism resumed in an Andean-type setting, with a significant increase in the portion of subaerial eruption products. Thus, the tectonic history of the UMVB includes at least two major stages. At present, this volcanic belt might comprise complexes produced by different tectonomagmatic systems.

(3) At least three compressional events of similar intensity took place at the observed segment of the Paleo-Pacific margin during the Cretaceous: pre-Aptian, early Albian, and late Turonian. These events might have been caused by the successive accretion of crustal blocks to the Siberian continent.

(4) Within the area of the present-day Ubienka River basin, the most obvious change in magma chemistry followed the pre-Aptian tectonic event, when the average SiO_2 content in the volcanics drastically increased, probably because of the wide-scale crustal melting. After the early Albian tectonic event, the increase in the average silica content in magmas was not significant, but the trace-element data indicate a slight change in the composition of the mantle protolith. Probably, a similar change occurred during the late Turonian tectonic event. To verify this suggestion, we need a more representative data set.

(5) The Turonian–Santonian strata of the Anadyr' segment of the OCVB bear signs of both along-strike and across-strike geochemical zonation. The general incompatible-element enrichment increases northeastward, following the changes of the basement complexes (from the juvenile terranes of the Oloi and South Anyui zones to the ancient crust of the Chukotka microcontinent), and northwestward, from frontal to back-arc zone of the OCVB.

The fieldwork was financially supported by the Georegion Federal State Unitary Geological Enterprise, Anadyr'. We thank A.B. Perepelov and V.V. Akinin for constructive reviews, which helped to improve the paper.

This work was partially supported by grants 16-05-00146 and 18-05-70011 from the Russian Foundation for Basic Research and by research program 0288-2017-0002 of the North-East Interdisciplinary Scientific Research Institute, Magadan.

REFERENCES

Akinin, V.V., Miller, E.L., 2011. Evolution of calc-alkaline magmas of the Okhotsk–Chukotka volcanic belt. Petrology 19 (3), 237–277.

Belyi, V.F., 1969. Volcanic Formations and Stratigraphy of the Northern Okhotsk–Chukotka Belt [in Russian]. Nauka, Moscow.

Belyi, V.F., 1975. Stratigraphy and age of volcanic deposits of the Okhotsk–Chukotka belt, in: The Mesozoic of the Northeastern USSR. Abstracts of the Interdepartmental Stratigraphic Workshop [in Russian]. Magadanskoe Knizhnoe Izdatel'stvo, Magadan, pp. 107–108.

Belyi, V.F., 1977. Stratigraphy and Structures of the Okhotsk–Chukotka Volcanic Belt [in Russian]. Nauka, Moscow.

Belyi, V.F., 1988. Relevant Issues of the Middle Cretaceous Phytostratigraphy of the Northeastern USSR [in Russian]. SVKNII DVNTs AN SSSR, Magadan.

Belyi, V.F., 2008. Talovka–Taigonos Euliminar System (Northeastern Russia) [in Russian]. SVKNII DVO AN SSSR, Magadan.

Belyi, V.F., Belaya, B.V., 1998. Late Evolution Stage of the Okhotsk–Chukotka Volcanic Belt (Upper Reaches of the Enmyvaam River) [in Russian]. SVKNII DVO AN SSSR, Magadan.

Bogdanov, A.A., 1965. Tectonic zoning of the Central Kazakhstan and Tien Shan Paleozoids. Paper 2. Variscan fold systems. Byulleten' MOIP. Ser. Geol. 40 (6), 8–38.

Bondarenko, G.E., Morozov, O.L., Layer, P., Minyuk, P.S., 1999. New Ar–Ar isotope dates for igneous and metamorphic rocks of the Taigonos Peninsula (northeastern Russia). Dokl. Akad. Nauk 369 (1), 76–83.

Bychkova, Ya.V., Sinitsyn, M.Yu., Petrenko, D.B., Nikolaeva, I.Yu., Bugaev, I.A., Bychkov, A.Yu., 2016. Specific technique of MS ICP multielement analysis of rocks. Vestnik MGU, Ser. 4. Geol., No. 6, 56–63.

Filatova, N.I., 1988. Perioceanic Volcanic Belts [in Russian]. Nedra, Moscow.

Fleck, R.J., Sutter, J.F., Elliot, D.H., 1977. Interpretation of discordant $^{40}Ar/^{39}Ar$ age spectra of Mesozoic tholeiites from Antarctica. Geochim. Cosmochim. Acta 41 (1), 15–32.

Frolova, T.I., Burikova, I.A., 1997. Igneous Rock Associations of Recent Geodynamic Settings [in Russian]. MGU, Moscow.

Gill, J.B., 1981. Orogenic Andesites and Plate Tectonics. Springer, New York.

Goryachev, N.A., 2005. The Uda–Murgal magmatic arc: geology, magmatism, and metallogeny, in: Metallogeny Problems of Ore Districts of Northeastern Russia [in Russian]. SVKNII DVO AN SSSR, Magadan, pp. 17–38.

Grantz, A., Hart, P.E., Childers, V.A., 2011. Geology and tectonic development of the Amerasia and Canada Basins, Arctic Ocean, in: Spencer, A.M., Embry, A.F., Gautier, D.L., Stoupakova, A.F., Sørensen, K. (Eds.), Arctic Petroleum Geology. Geol. Soc. London Mem. 35, 771–799.

Gustafson, L.B., Orquera, W., McWillian, M., Castro, M., Olivares, O., Rojas, G., Maluenda, J., Mendez, M., 2001. Multiple centers of mineralization in the Indio Muerto District, El Salvador, Chile. Econ. Geol. 96, 325–350.

James, D.E., Sacks, I.S., 1999. Cenozoic formation of the Central Andes: a geophysical perspective, in: Skinner, B.J. (Ed.), Geology and Ore Deposits of the Central Andes. Soc. Econ. Geol. Spec. Publ. 7, 1–25.

Khanchuk, A.I. (Ed.), 2006. Geodynamics, Magmatism, and Metallogeny of Eastern Russia [in Russian]. Dal'nauka, Vladivostok.

Kotlyar, I.N., Belyi, V.F., Milov, A.P., 1981. Petrochemistry of Igneous Rock Associations of the Okhotsk–Chukotka Volcanic Belt [in Russian]. Nauka, Moscow.

Larionov, A.N., Andreichev, V.A., Gee, D.G., 2004. The Vendian alkaline igneous suite of northern Timan: ion microprobe U–Pb zircon ages of gabbros and syenite, in: Gee, D.G., Pease, V. (Eds.). The Neoproterozoic Timanide Orogen of Eastern Baltica. Geol. Soc. London Mem. 30, 69–74.

Le Maitre, R.W., 1989. A Classification of Igneous Rocks and Glossary of Terms: Recommendations of the International Union of Geological Sciences Subcommission on the Systematics of Igneous Rocks. Blackwell Scientific, Oxford.

Lobunets, S.S., Kuznetsova, I.A., 1977. State Geological Map of the USSR, Scale 1 : 200,000. Eropol' Series. Sheet P-58-VI. Explanatory Note [in Russian]. Kartfabrika Ob''edineniya "Aerogeologiya", Leningrad.

Luchitskaya, M.V., Hourigan, J., Bondarenko, G.E., 2003. New SHRIMP U–Pb zircon data on granitoids from the Pribrezhnyi and Eastern Taigonos belts, southern Taigonos Peninsula. Dokl. Earth Sci. 389A (3), 354–357.

Ludwig, K.R., 2005a. SQUID 1.12. A User's Manual. A Geochronological Toolkit for Microsoft Excel. Berkeley Geochronology Center Special Publication.

Ludwig, K.R., 2005b. User's Manual for ISOPLOT/Ex 3.22. A Geochronological Toolkit for Microsoft Excel. Berkeley Geochronology Center Special Publication.

Makhonina, L.I., Bakai, G.G., 1979. State Geological Map of the USSR, Scale 1 : 200,000. Eropol' Series. Sheet P-58-IX. Explanatory Note [in Russian]. Kartfabrika Ob''edineniya "Aerogeologiya", Leningrad.

Malysheva, G.M., Isaeva, E.P., Tokhomirov, Yu.B., Vyatkin, B.V., 2012. State Geological Map of the Russian Federation (New Series), Scale 1 : 1,000,000 (Third Generation). Chukotka Series. Sheet Q-59 (Markovo). Explanatory Note [in Russian]. Kartfabrika VSEGEI, St. Petersburg.

Miller, E.L., Toro, J., Gehrels, G., Amato, J.M., Prokopiev, A.V., Tuchkova, M.I., Akinin, V.V., Dumitru, T.A., Moore, T.E., Cecile, M.P., 2006. New insights into Arctic paleogeography and tectonics from U–Pb detrital zircon geochronology. Tectonics 25 (3), p. TC3013.

Moiseev, A.V., 2015. Structure and Tectonic Evolution of the Ust'-Belaya Segment of the West Koryak Fold System (Northeastern Russia, Koryakia). PhD Thesis [in Russian]. Moscow.

Montin, S.A., 1992. Fold–thrust dislocations of the Upper Cretaceous volcanics of the Okhotsk–Chukotka volcanic belt. Vestnik MGU, Ser. 4. Geol., No. 2, 88–91.

Morozov, O.L., 2001. Geologic Structure and Tectonic Evolution of the Central Chukotka Region [in Russian]. GEOS, Moscow.

Nekrasov, G.E., 1976. Tectonics and Magmatism of the Taigonos Peninsula and Northwestern Kamchatka Region [in Russian]. Nauka, Moscow.

Nevretdinov, E.B., 1985. State Geological Map of the USSR, Scale 1 : 200,000. Eropol' Series. Sheet Q-59-XXV–Q-59-XXVI. Explanatory Note [in Russian]. Soyuzgeolfond, Moscow.

Nokleberg, W.J., Parfenov, L.M., Monger, J.W.H., Norton, I.O., Khanchuk, A.I., Stone, D.B., Scotese, C.R., Scoll, D.W., Fujita, K., 2001. Phanerozoic Tectonic Evolution of the Circum–North Pacific. US Geological Survey Professional Paper 1626.

Ogg, J.G., Ogg, G., Gradstein, F.M., 2008. The Concise Geologic Time Scale. Cambridge University Press, New York.

Parfenov, L.D., 1984. Continental Margins and Island Arcs of the Mesozoids in Northeastern Asia [in Russian]. Nauka, Novosibirsk.

Resolutions of the Third Interdepartmental Regional Stratigraphic Workshop on the Precambrian, Paleozoic, and Mesozoic of Northeastern Russia (St. Petersburg, 2002) [in Russian], 2009. Izd. VSEGEI, St. Petersburg.

Rudnick, R.L., Gao, S., 2004. Composition of the continental crust, in: Holland, H.D., Turekian, K.K. (Eds.). Treatise on Geochemistry. Elsevier, Amsterdam, Vol. 3. pp. 1–64.

Rusakova, T.B., 2011. Late Jurassic–Neocomian volcanism of the northern Okhotsk region: geology, tectonic settings, and mineralization. Russ. J. Pacific Geol. 5 (5), 418–432.

Shibata, T., Nakamura, E., 1997. Across-arc variations of isotope and trace element compositions from Quaternary basaltic volcanic rocks in northeastern Japan: implications for interaction between subducted oceanic slab and mantle wedge. J. Geophys. Res. 102 (B4), 8051–8064.

Shpetnyi, A.P., Ichetovkin, N.V., Kaigorodtsev, G.G., 1974. Igneous rock complexes of the northeastern USSR and their location in geologic structures, in: Magmatism of Northeastern Asia. Proceedings of the First Northeastern Petrographic Workshop [in Russian]. Magadanskoe Knizhnoe Izd., Magadan, Part 1, pp. 25–38.

Sokolov, S.D., Bondarenko, G.Ye., Khudoley, A.K., Morozov, O.L., Luchitskaya, M.V., Tuchkova, M.I., Layer, P.W., 2009. Tectonic reconstruction of Uda–Murgal arc and the Late Jurassic and Early Cretaceous convergent margin of Northeast Asia–Northwest Pacific, in: Geology, Geophysics and Tectonics of Northeastern Russia: A Tribute to Leonid Parfenov. Stephan Mueller Spec. Publ. Ser. 4, pp. 273–288.

Steiger, R.H., Jager, E., 1977. Subcommission on Geochronology: Convention on the use of decay constants in geo- and cosmochronology. Earth Planet. Sci. Lett. 36 (3), 359–362.

Sun, S.-S., McDonough, W.F., 1989. Chemical and isotopic systematic of oceanic basalts: implications for mantle composition and processes, in: Saunders, A.D., Norry, M.J. (Eds.). Magmatism in the Ocean Basins. Geol. Soc. London Spec. Publ. 42, 313–345.

Tatsumi, Y., Eggins, S., 1995. Subduction Zone Magmatism (Frontiers in Earth Sciences). Blackwell Science, Oxford.

Tikhomirov, P.L., Kalinina, E.A., Kobayashi, K., Nakamura, E., 2008. Late Mesozoic silicic magmatism of the North Chukotka area (NE Russia): age, magma sources, and geodynamic implications. Lithos 105, 329–346.

Tikhomirov, P.L., 2010. Large Phanerozoic silicic-volcanism provinces: geodynamic settings and formation conditions. Vestnik MGU, Ser. 4. Geol., No. 3, 42–50.

Tikhomirov, P.L., 2018. Cretaceous Continent-Marginal Magmatism of Northeastern Asia and Genesis of Large Phanerozoic Silicic-Volcanism Provinces. ScD Thesis [in Russian]. MGU, Moscow.

Tikhomirov, P.L., Kalinina, E.A., Moriguti, T., Makishima, A., Kobayashi, K., Cherepanova, I.Yu., Nakamura, E., 2012. The Cretaceous Okhotsk–Chukotka Volcanic Belt (NE Russia): geology, geochronology, magma output rates, and implications on the genesis of silicic LIPs. J. Volcanol. Geotherm. Res. 221–222, 14–32.

Tikhomirov, P.L., Kalinina, E.A., Moriguti, T., Makishima, A., Kobayashi, K., Nakamura, E., 2016. Trace element and isotopic geochemistry of Cretaceous magmatism in NE Asia: Spatial zonation, temporal evolution, and tectonic controls. Lithos 264, 453–471.

Travin, A.V., Yudin, D.S., Vladimirov, A.G., Khromykh, S.V., Volkova, N.I., Mekhonoshin, A.S., Kolotilina, T.B., 2009. Thermochronology of the Chernorud granulite zone, Ol'khon region, western Baikal area. Geol. Int. 47 (11), 1107–1124.

Trunov, B.D., 1977. Geological Map of the USSR, Scale 1 : 200,000. Anadyr' Series. Sheet Q-59-XXI–Q-59-XXII [in Russian]. Kartfabrika VAGT, Leningrad.

Umitbaev, R.B., 1986. The Okhotsk–Chaun Metallogenic Province [in Russian]. Nauka, Moscow.

Ustiev, E.K., 1959. The Okhotsk tectono-magmatic belt and associated problems. Sovetskaya Geologiya, No. 3, 3–26.

Ustiev, E.K., 1963. The Okhotsk structural belt and problems of volcanoplutonic formations, in: Magma Problems and Genesis of Igneous Rocks [in Russian]. Izd. AN SSSR, Moscow, pp. 161–182.

Wiedenbeck, M., Allé, P., Corfu, F., Griffin, W.L., Meier, M., Oberli, F., Von Quadt, A., Roddick, J.C., Spiegel, W., 1995. Three natural zircon standards for U–Th–Pb, Lu–Hf, trace element and REE analysis. Geostand. Newslett. 19, 1–23.

Wilson, M., 1989. Igneous Petrogenesis: A Global Tectonic Approach. Unwin Hyman, London.

Zhou, Y., Liang, X., Kröner, A., Cai, Y., Shao, T., Wen, S., Jiang, Y., Fu, J., Wang, C., Dong, C., 2015. Late Cretaceous lithospheric extension in SE China: Constraints from volcanic rocks in Hainan Island. Lithos 232, 100–110.

Editorial responsibility: A.E. Izokh